US 20160036225A1

(19) **United States**
(12) **Patent Application Publication**
(10) **Pub. No.: US 2016/0036225 A1**
(43) **Pub. Date: Feb. 4, 2016**

Zhao et al.

(54) **DYNAMIC FREQUENCY CONTROL IN POWER NETWORKS**

(71) Applicant: **California Institute of Technology**, Pasadena, CA (US)

(72) Inventors: **Changhong Zhao**, Pasadena, CA (US); **Enrique Mallada Garcia**, Pasadena, CA (US); **Steven H. Low**, La Canada, CA (US)

(73) Assignee: **California Institute of Technology**, Pasadena, CA (US)

(21) Appl. No.: **14/796,869**

(22) Filed: **Jul. 10, 2015**

Related U.S. Application Data

(60) Provisional application No. 62/022,861, filed on Jul. 10, 2014.

Publication Classification

(51) **Int. Cl.**
H02J 3/00 (2006.01)
G05B 13/04 (2006.01)

(52) **U.S. Cl.**
CPC ***H02J 3/00*** (2013.01); ***G05B 13/041*** (2013.01)

(57) **ABSTRACT**

Node controllers in power distribution networks in accordance with embodiments of the invention enable dynamic frequency control. One embodiment includes a node controller comprising a network interface a processor; and a memory containing a frequency control application; and a plurality of node operating parameters describing the operating parameters of a node, where the node is selected from a group consisting of at least one generator node in a power distribution network wherein the processor is configured by the frequency control application to calculate a plurality of updated node operating parameters using a distributed process to determine the updated node operating parameter using the node operating parameters, where the distributed process controls network frequency in the power distribution network; and adjust the node operating parameters.

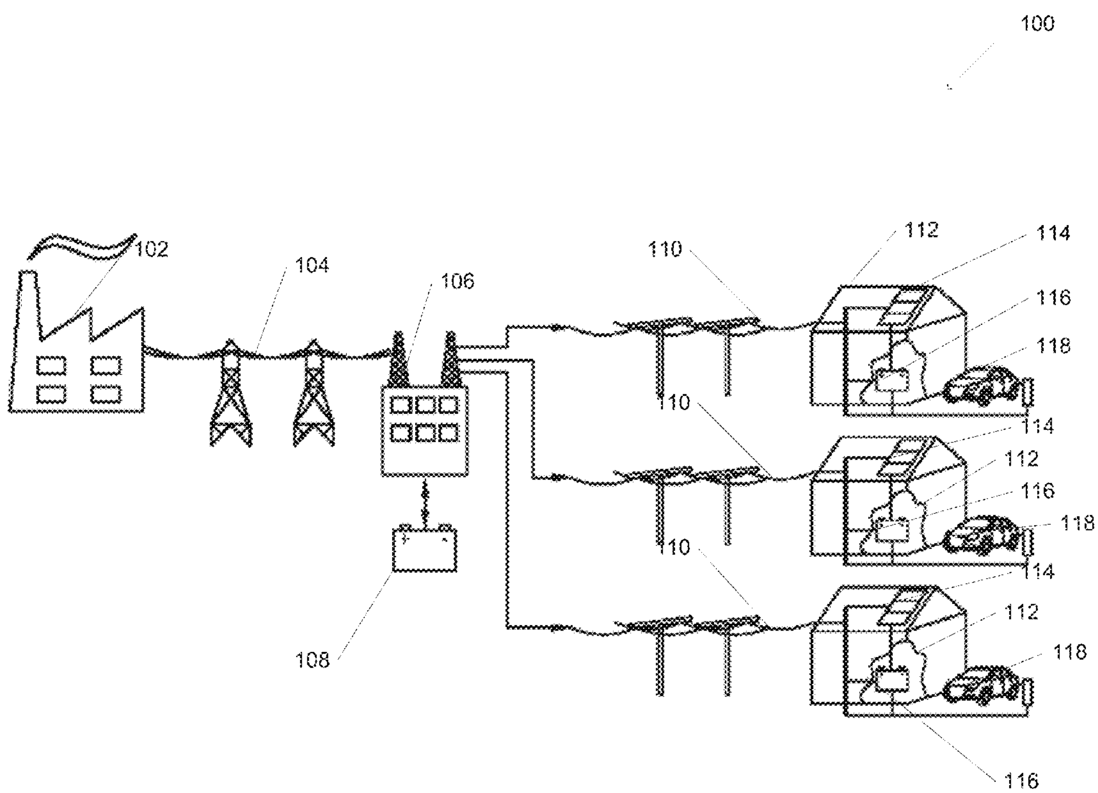

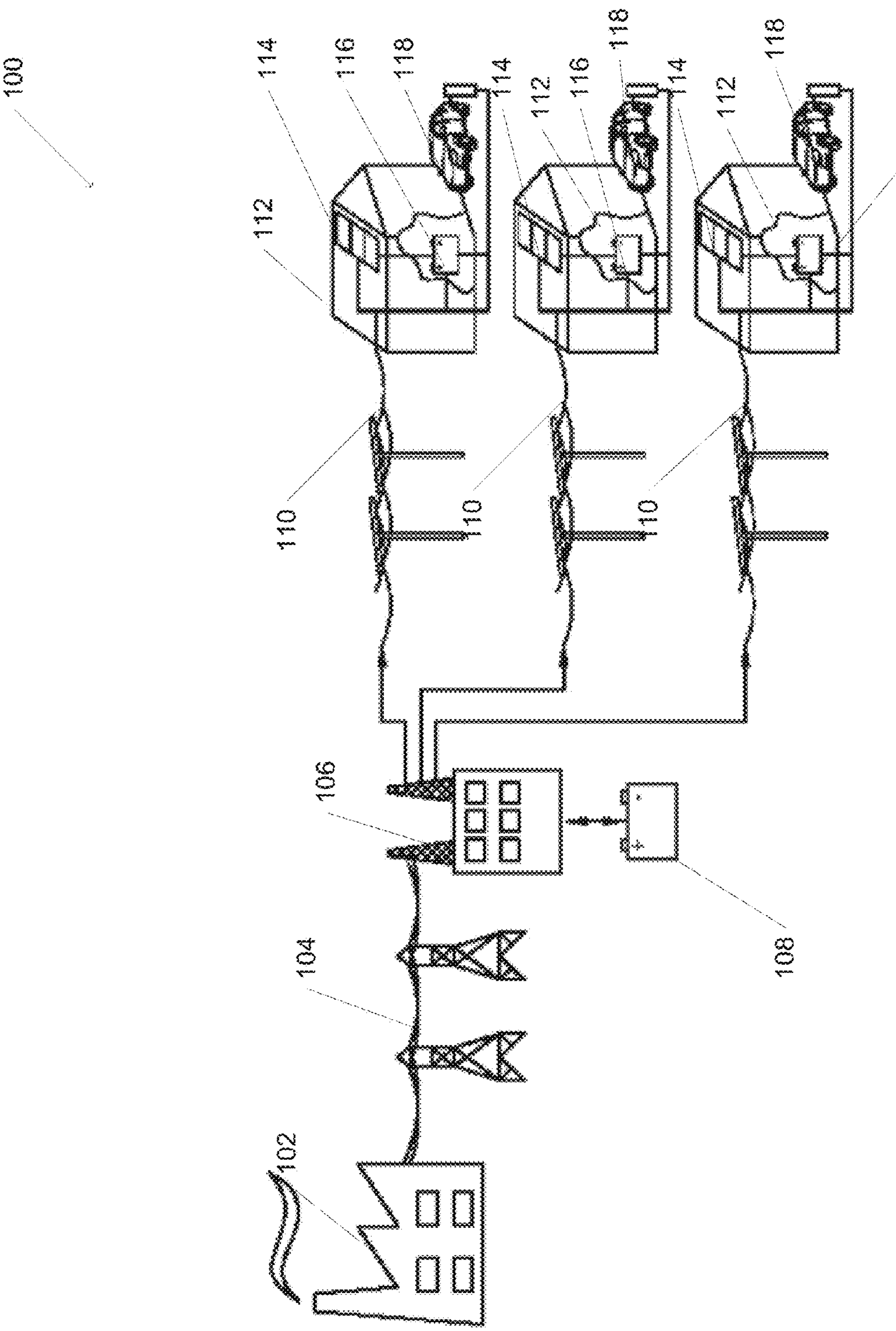

FIG. 1

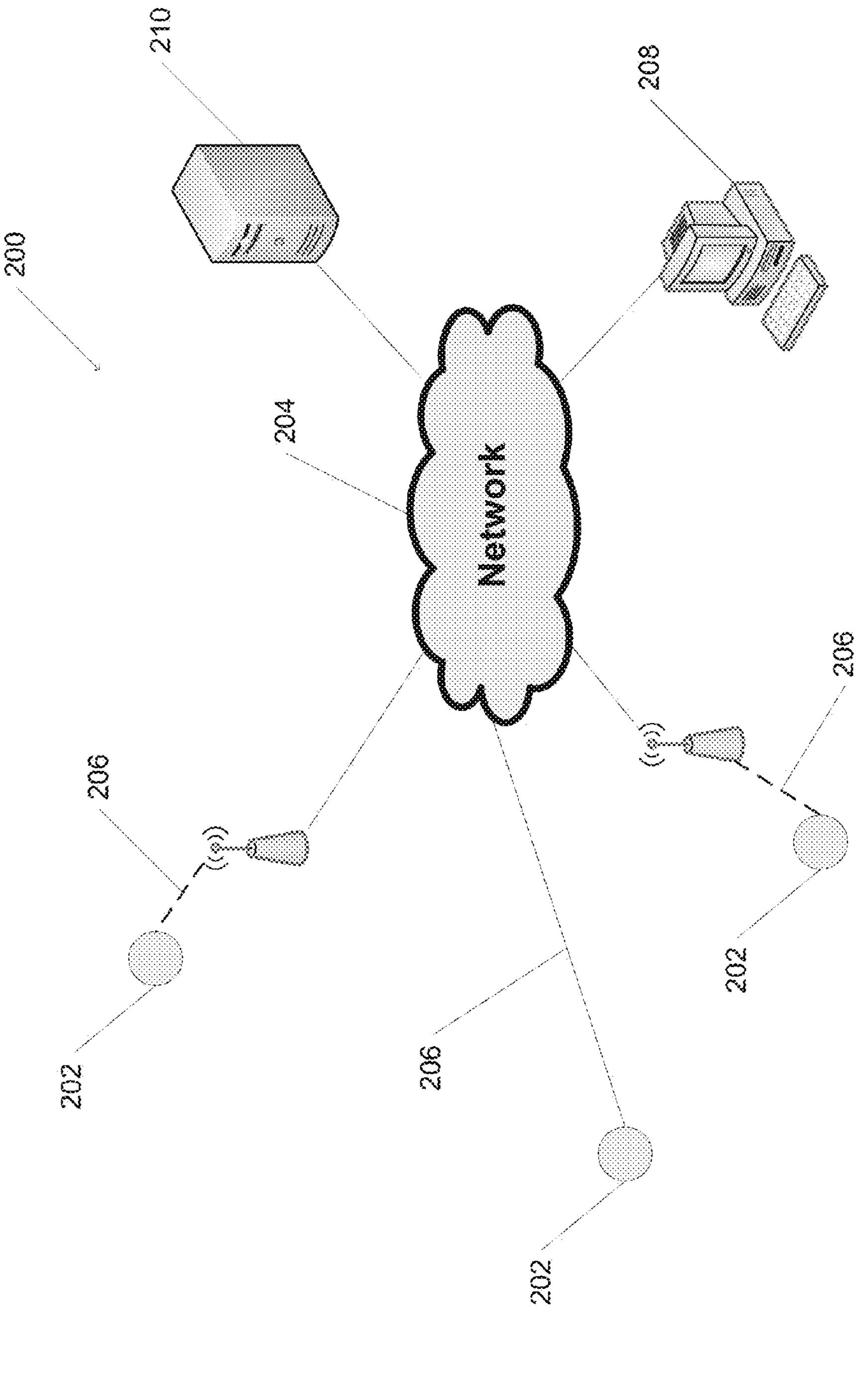

FIG. 2

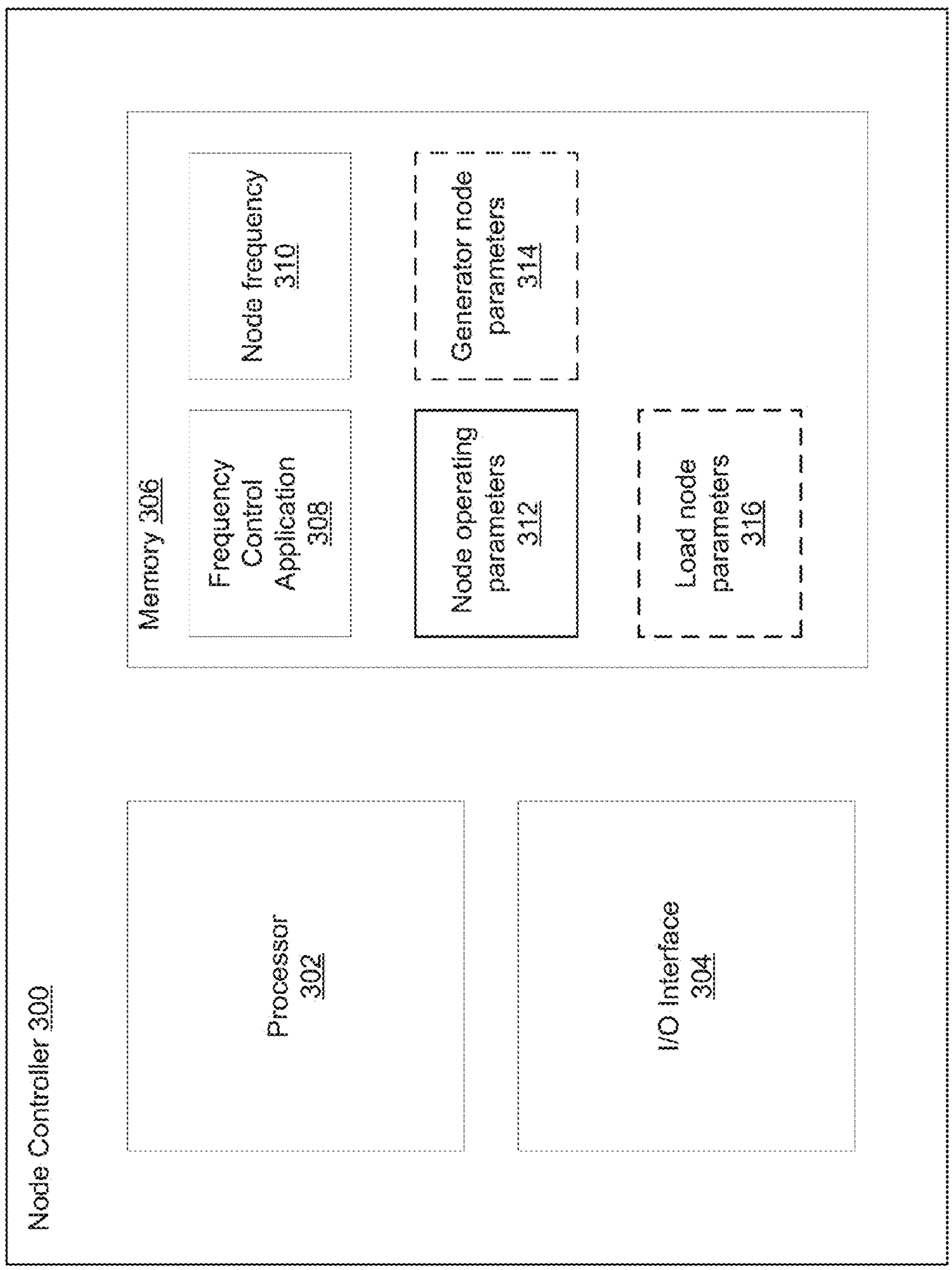
Node Controller 300
Processor 302
I/O Interface 304
Memory 306
Frequency Control Application 308
Node frequency 310
Node operating parameters 312
Generator node parameters 314
Load node parameters 316

FIG. 3

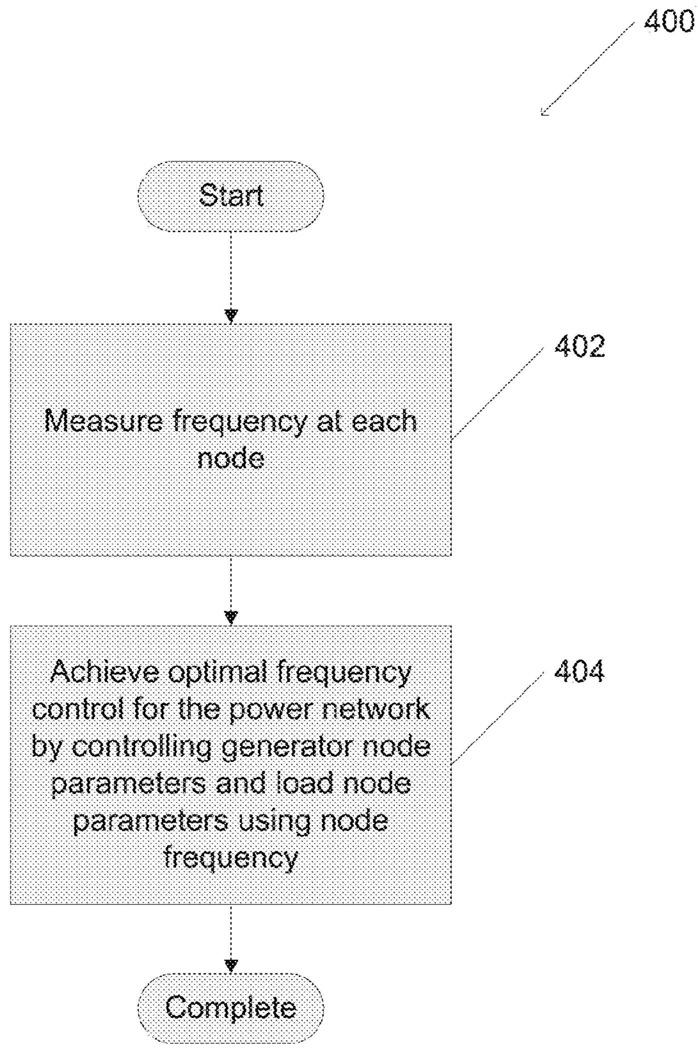
400
Start
Measure frequency at each node
402
Achieve optimal frequency control for the power network by controlling generator node parameters and load node parameters using node frequency
404
Complete

FIG. 4

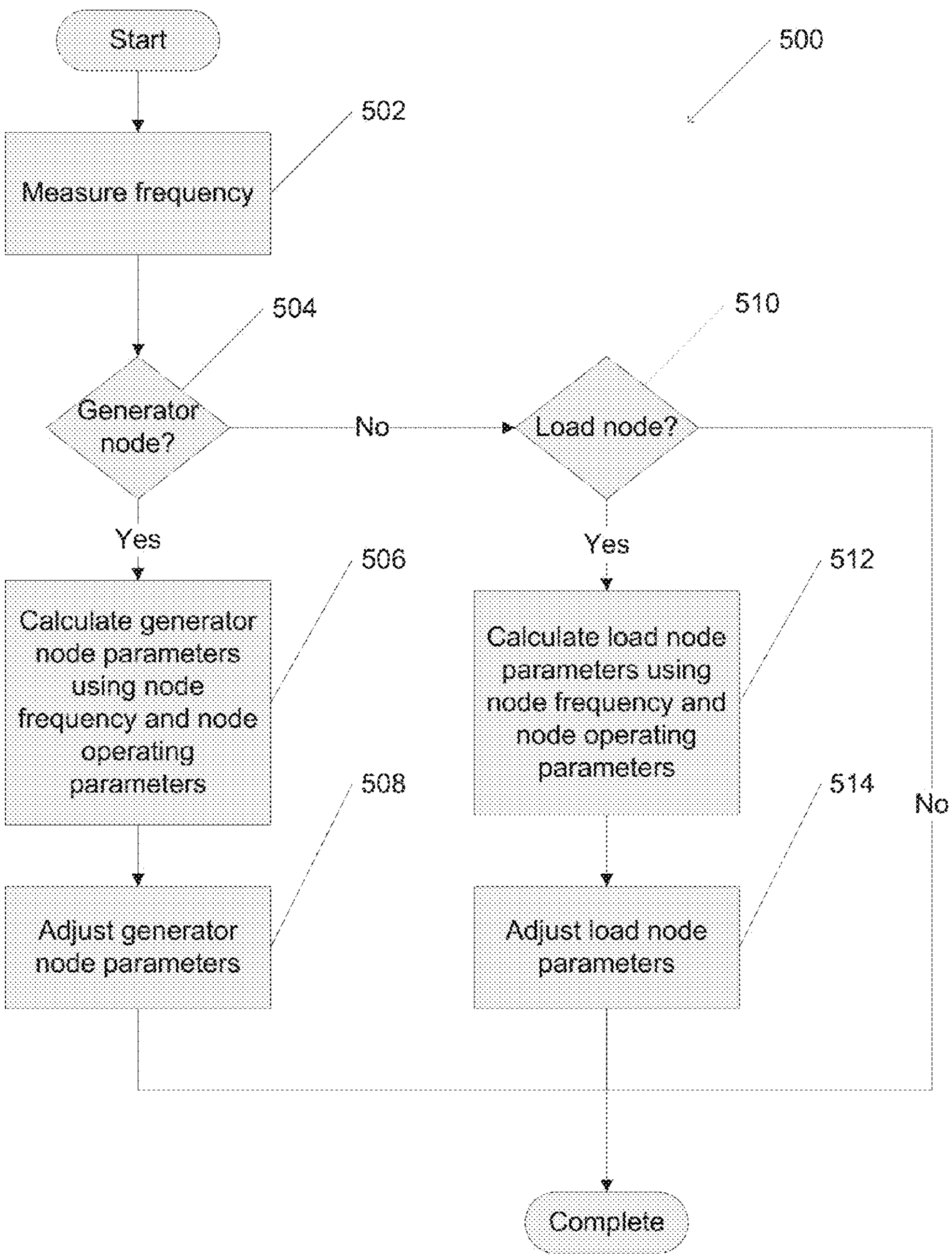
500
Start
502
Measure frequency
504
Generator node?
No
510
Load node?
Yes
506
Calculate generator node parameters using node frequency and node operating parameters
508
Adjust generator node parameters
Yes
512
Calculate load node parameters using node frequency and node operating parameters
514
Adjust load node parameters
No
Complete

FIG. 5

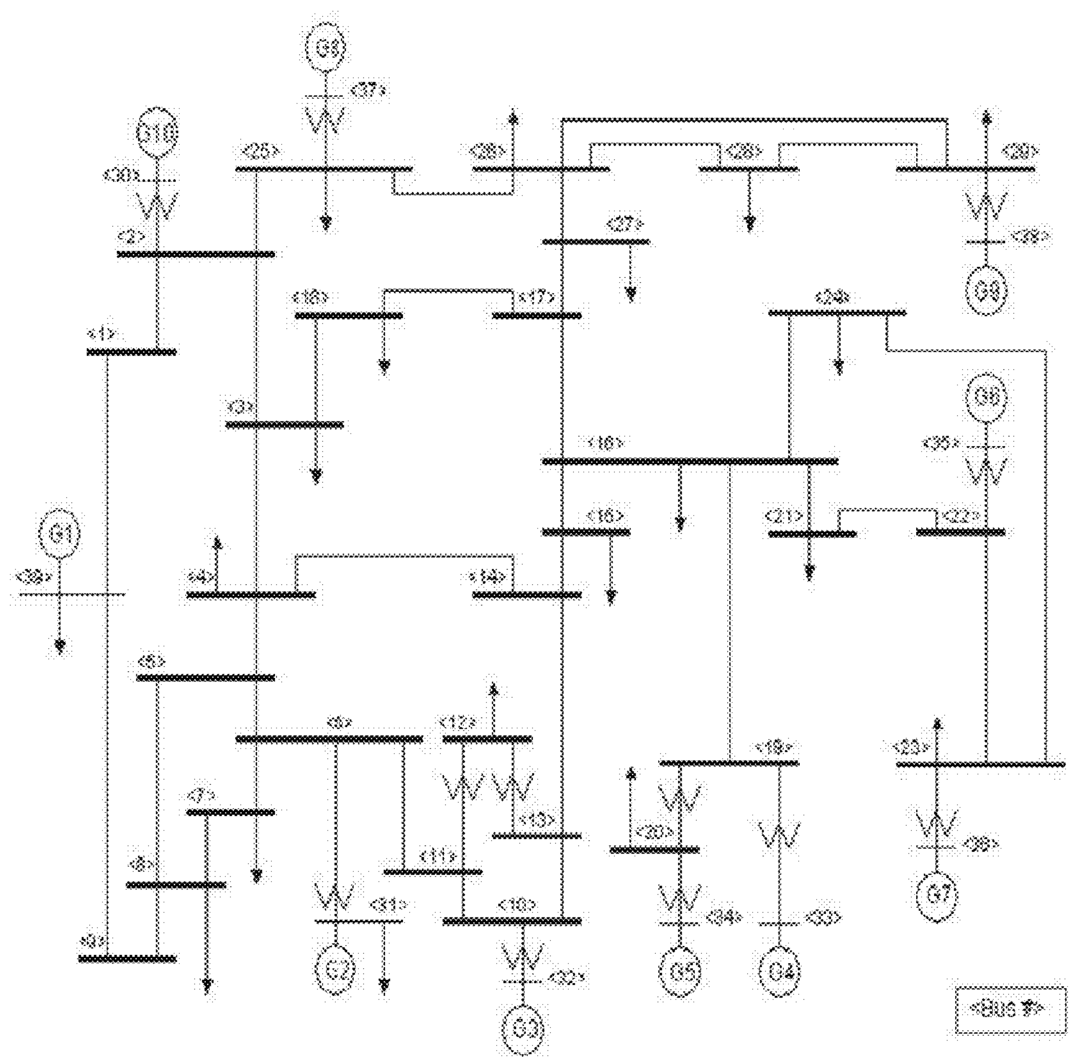

FIG. 6

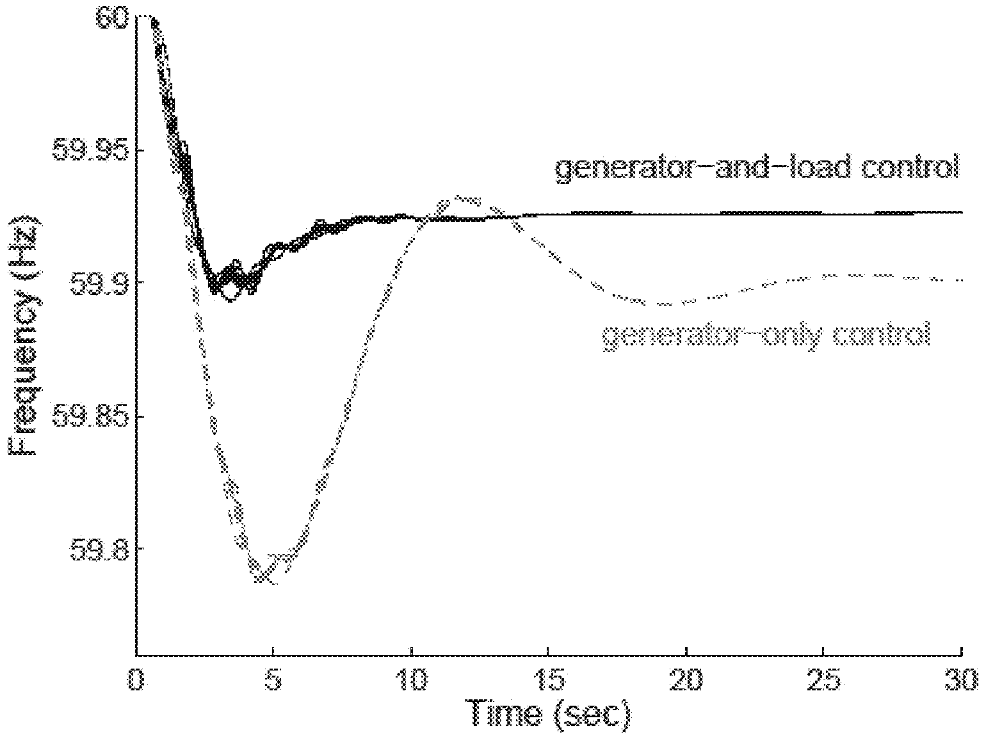
60
59.95
59.9
59.85
59.8
Frequency (Hz)
generator-and-load control
generator-only control
0
5
10
15
20
25
30
Time (sec)

FIG. 7

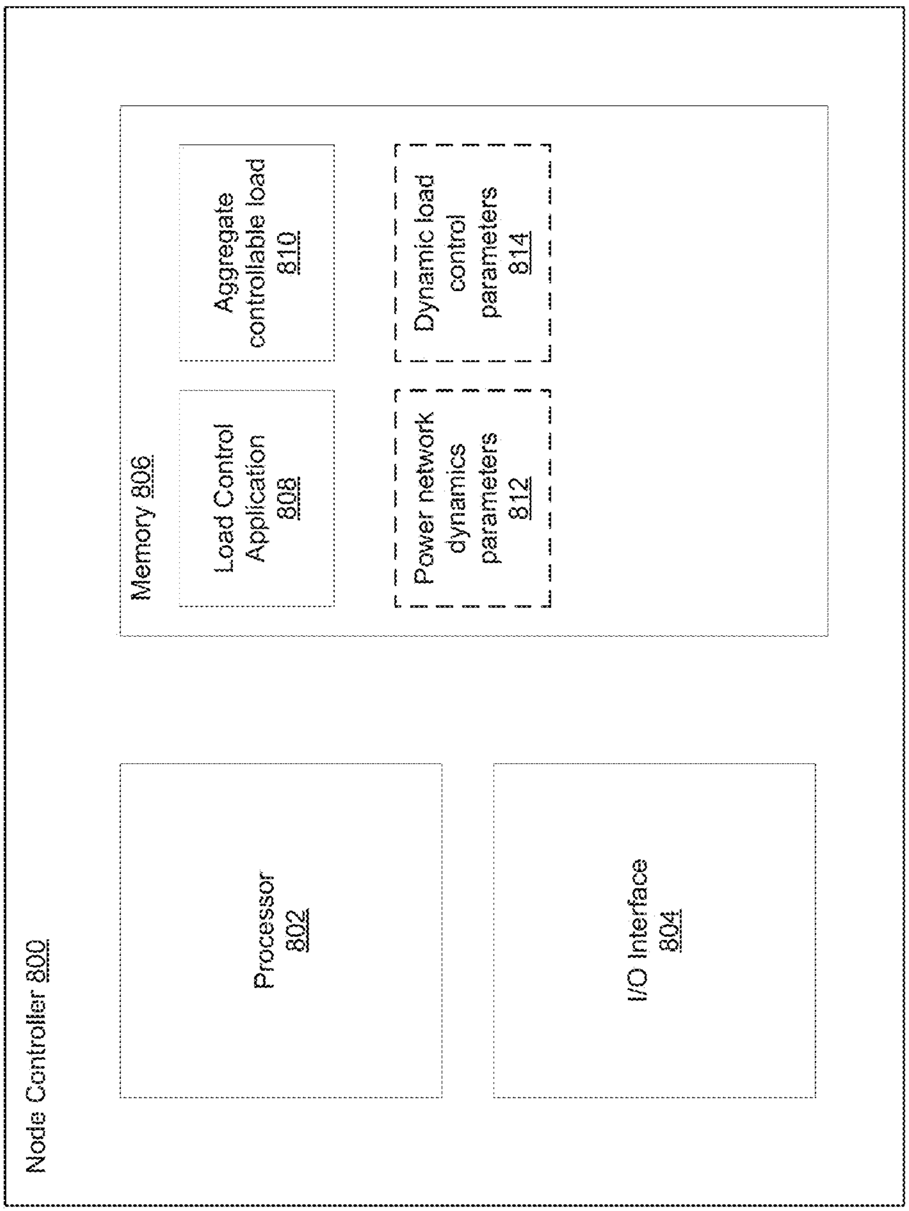
Node Controller 800
Processor 802
I/O Interface 804
Memory 806
Load Control Application 808
Aggregate controllable load 810
Power network dynamics parameters 812
Dynamic load control parameters 814

FIG. 8

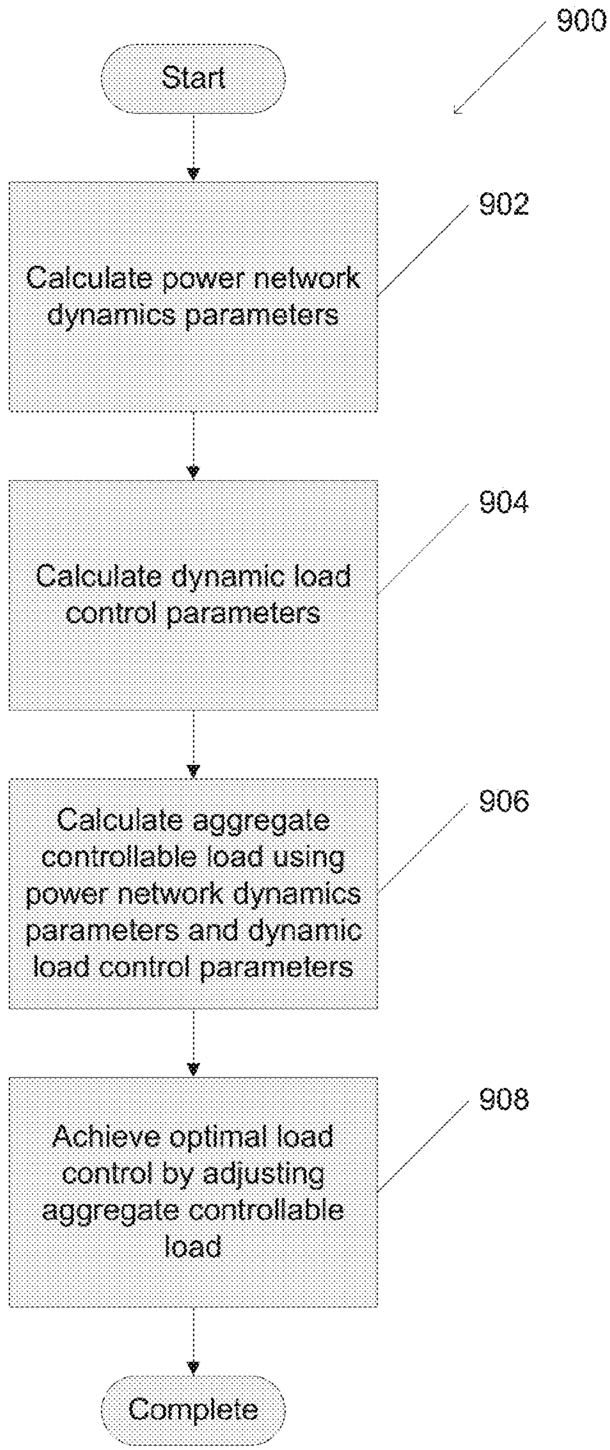
900
Start
Calculate power network dynamics parameters
902
Calculate dynamic load control parameters
904
Calculate aggregate controllable load using power network dynamics parameters and dynamic load control parameters
906
Achieve optimal load control by adjusting aggregate controllable load
908
Complete

FIG. 9

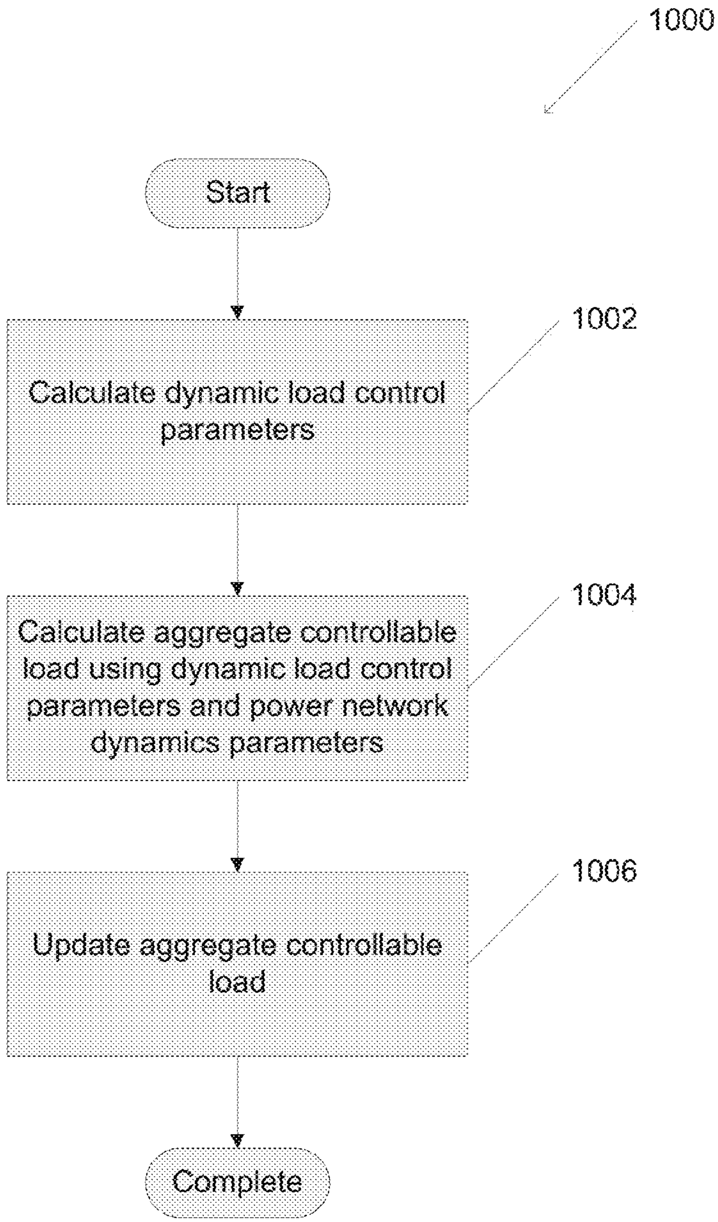
1000
Start
Calculate dynamic load control parameters
1002
Calculate aggregate controllable load using dynamic load control parameters and power network dynamics parameters
1004
Update aggregate controllable load
1006
Complete

FIG. 10

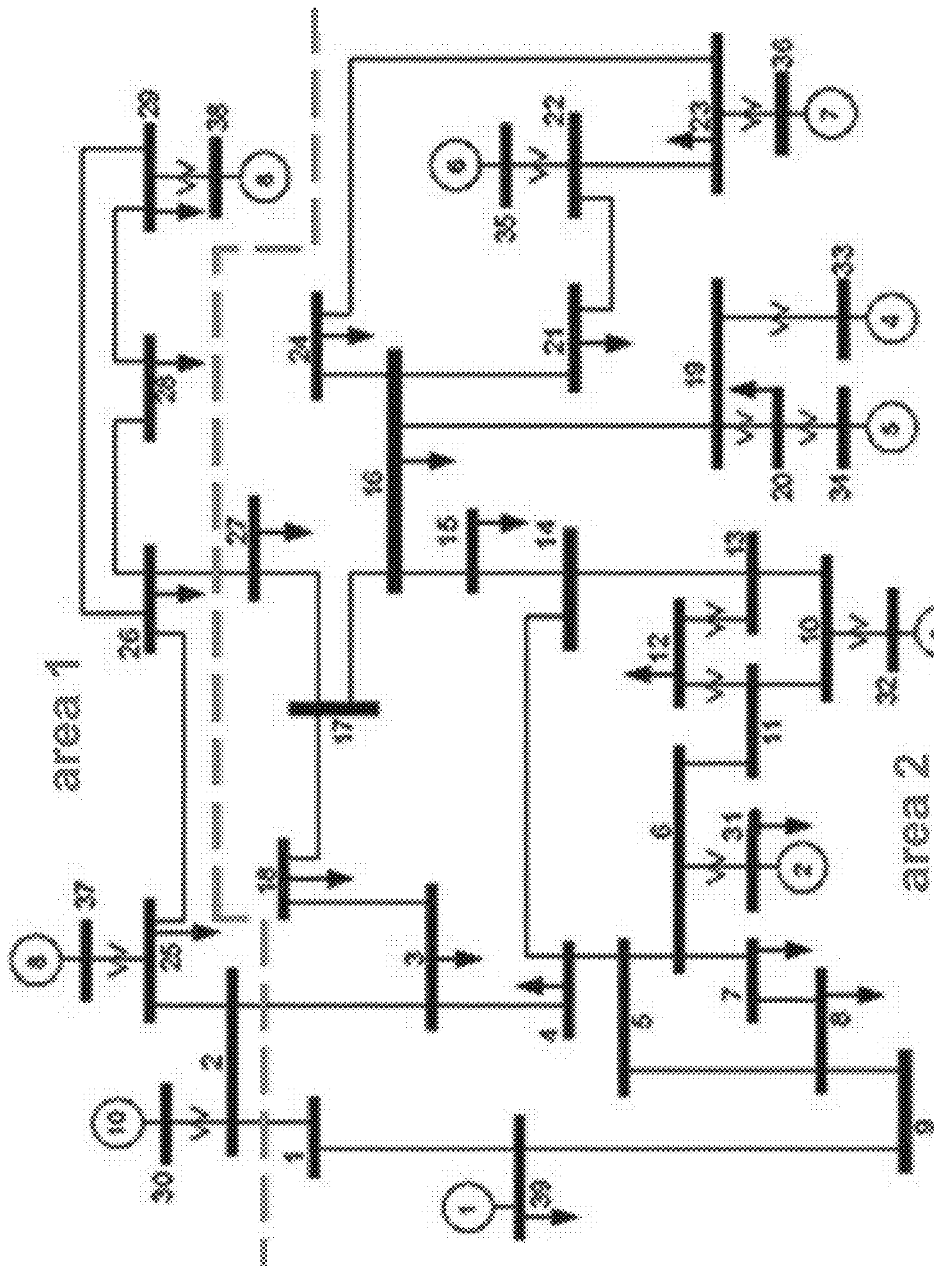

FIG. 11

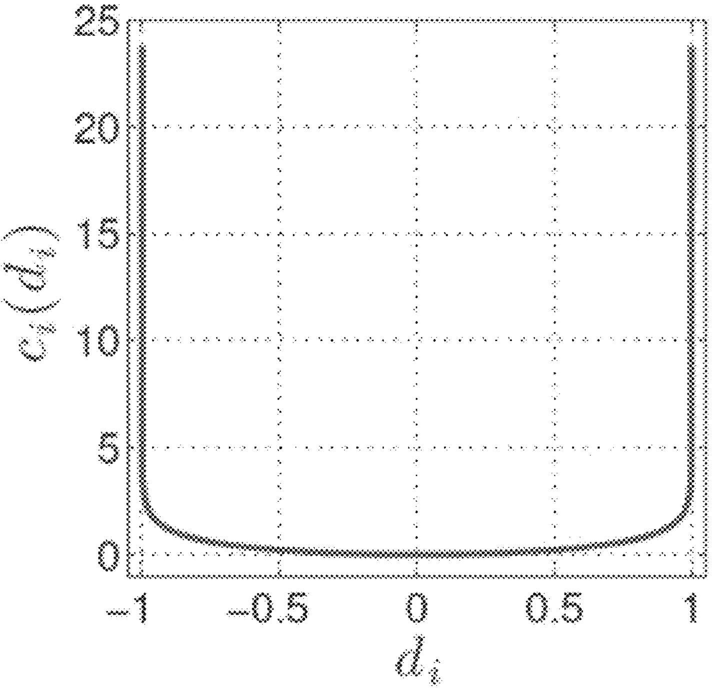

FIG. 12A

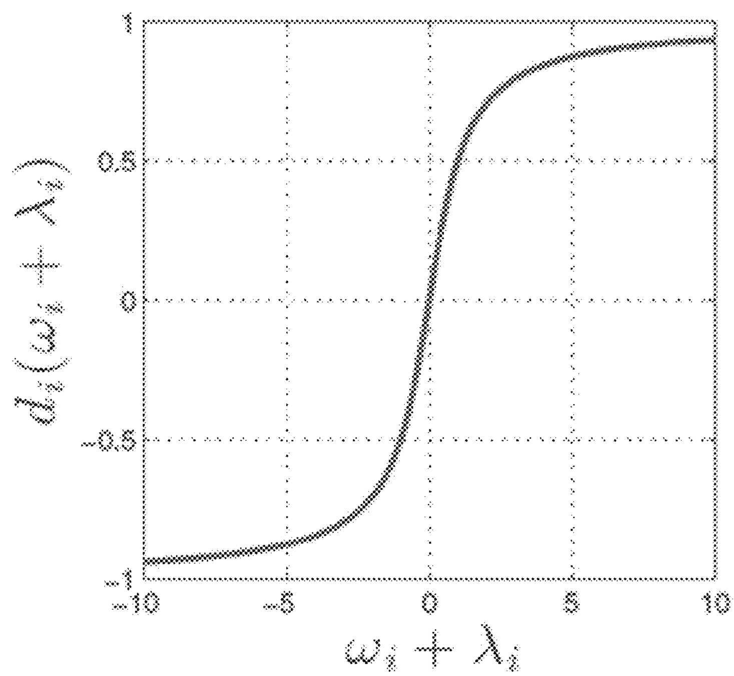

FIG. 12B

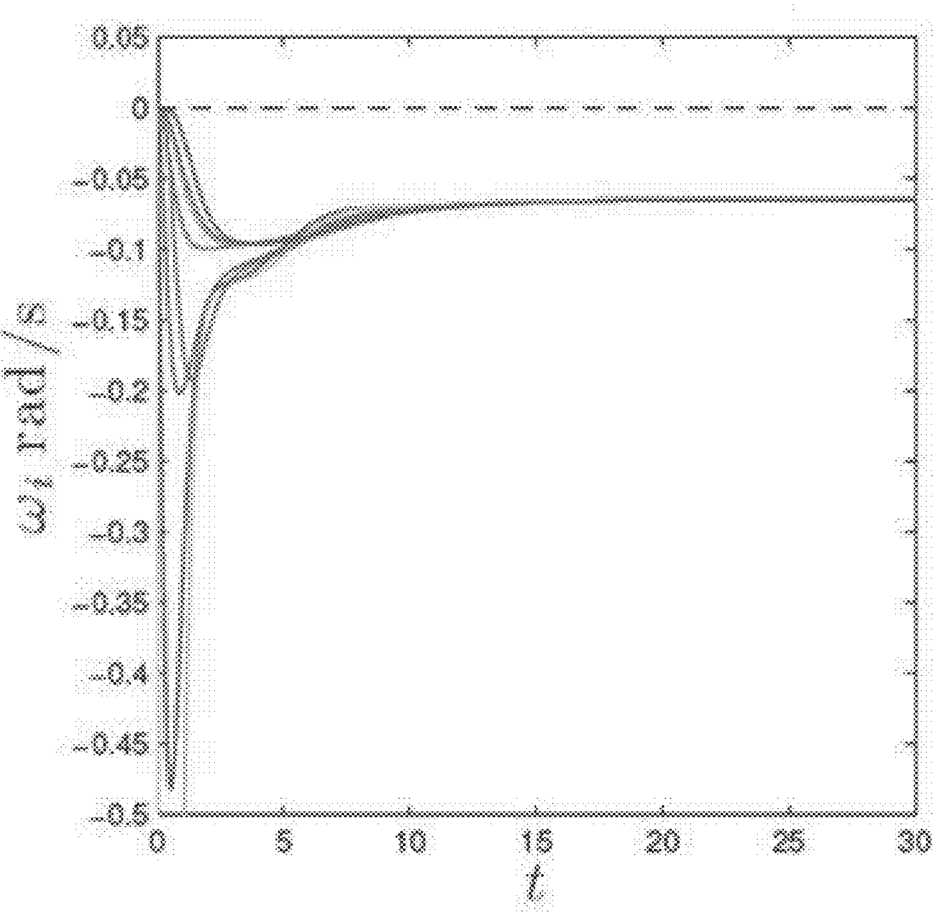
0.05
0
−0.05
−0.1
−0.15
−0.2
−0.25
−0.3
−0.35
−0.4
−0.45
−0.5
ω_i rad/s
0
5
10
15
20
25
30
t

FIG. 13A

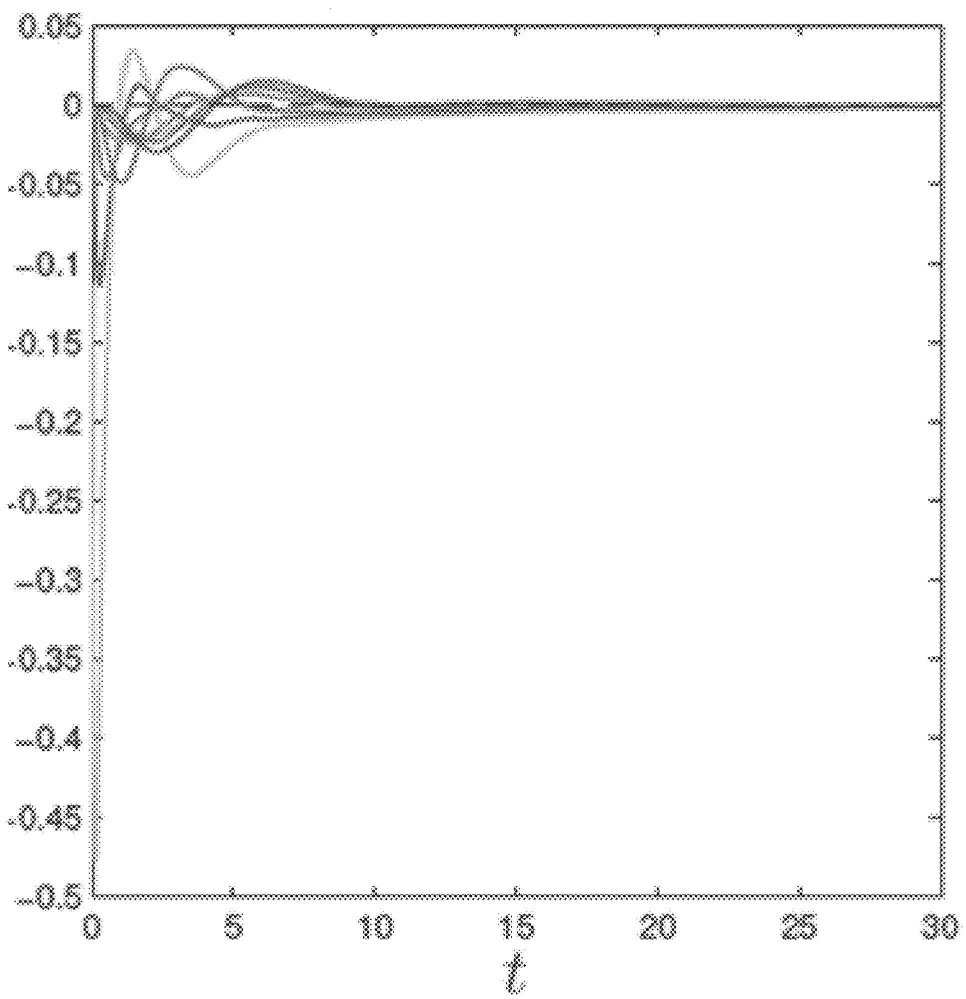

FIG. 13B

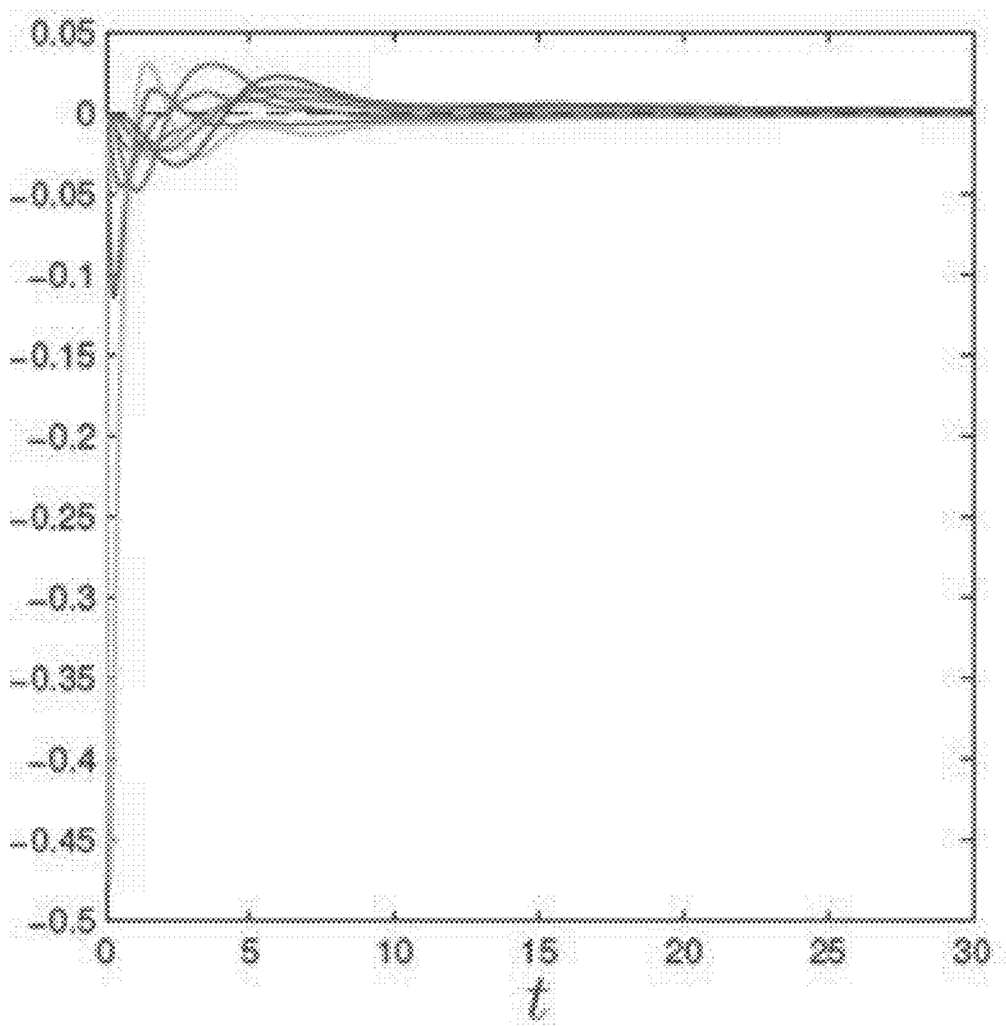

FIG. 13C

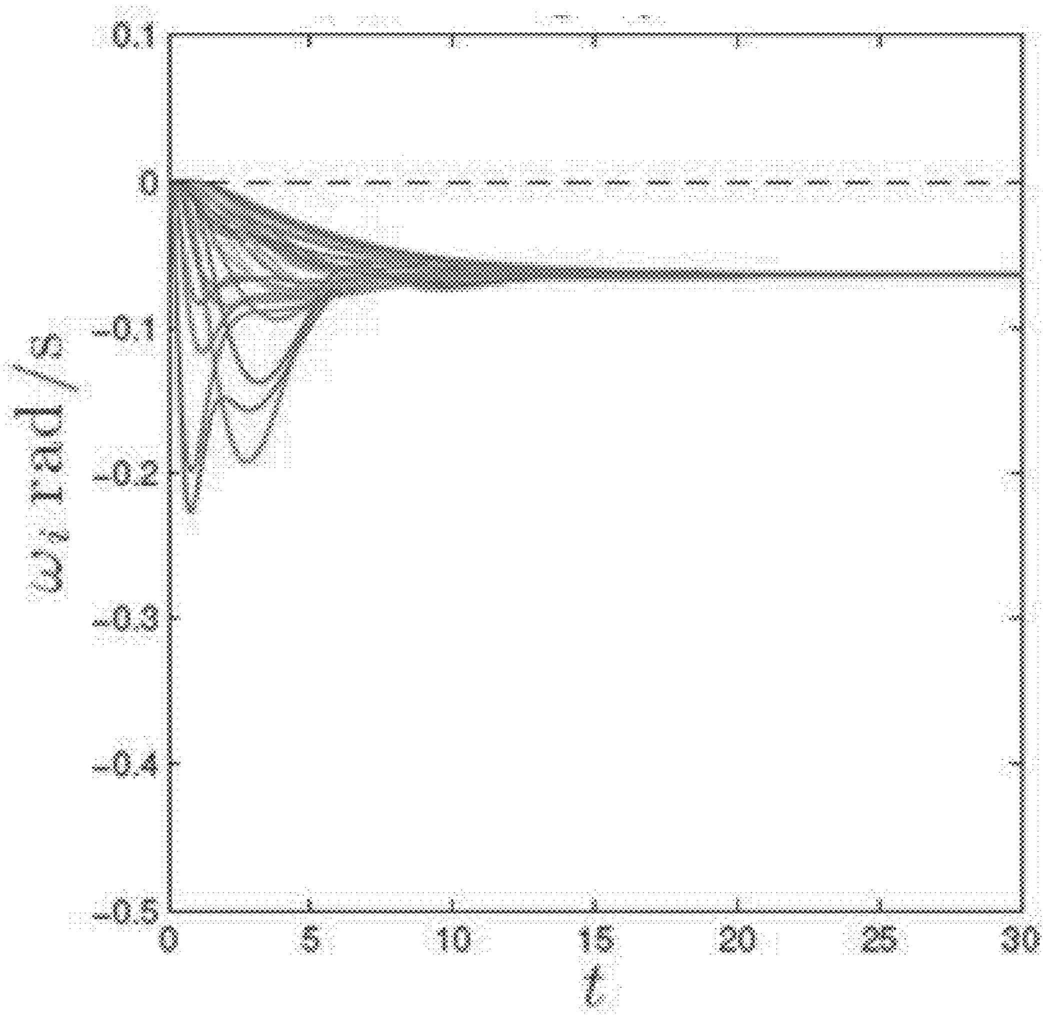

FIG. 14A

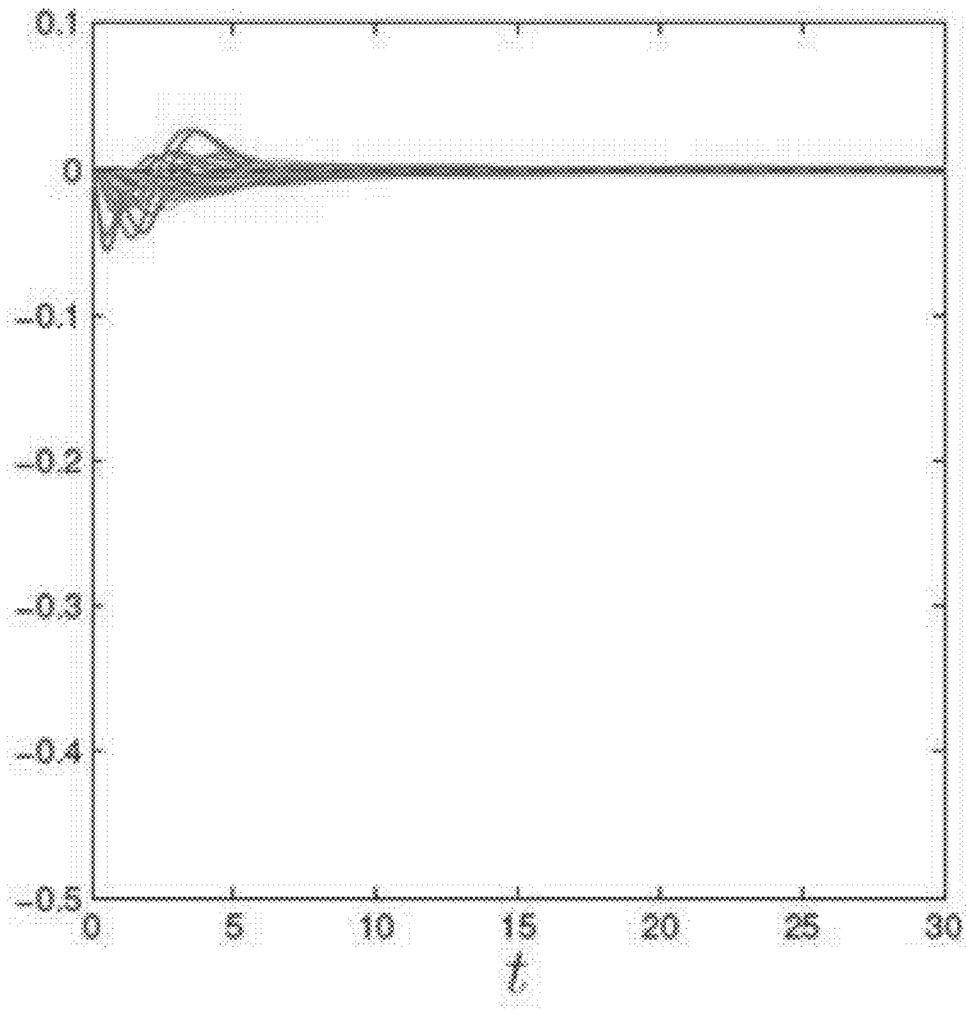

FIG. 14B

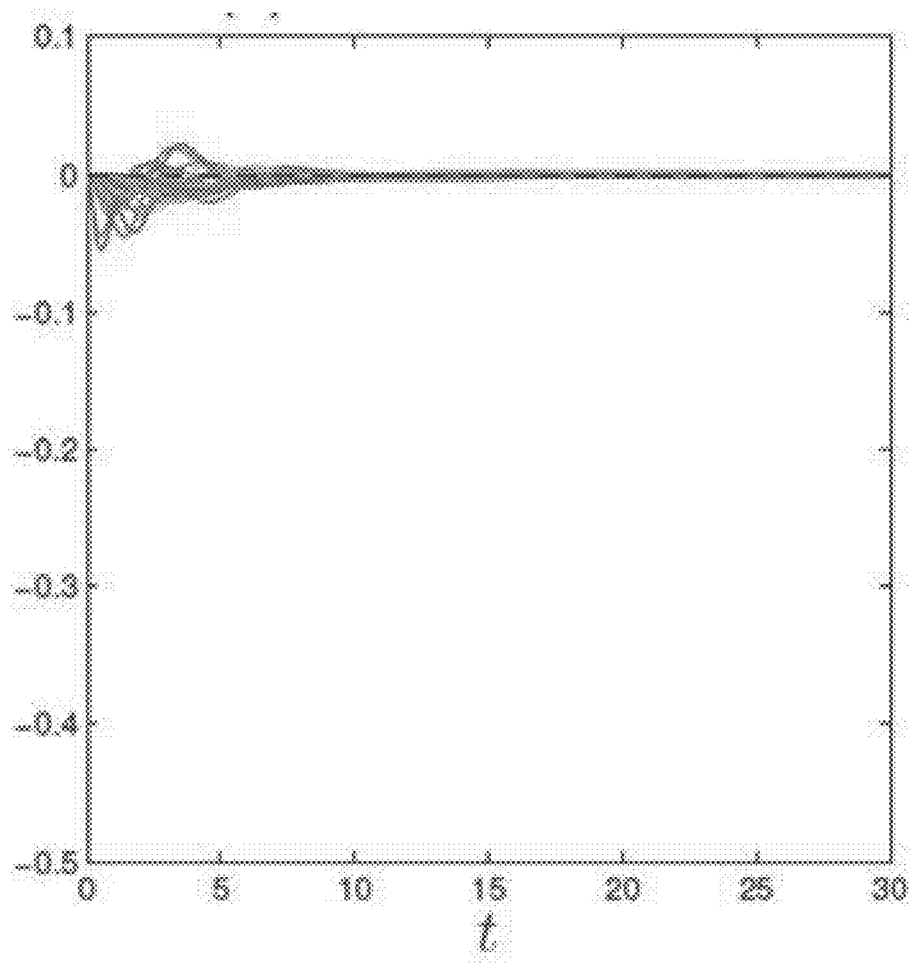

FIG. 14C

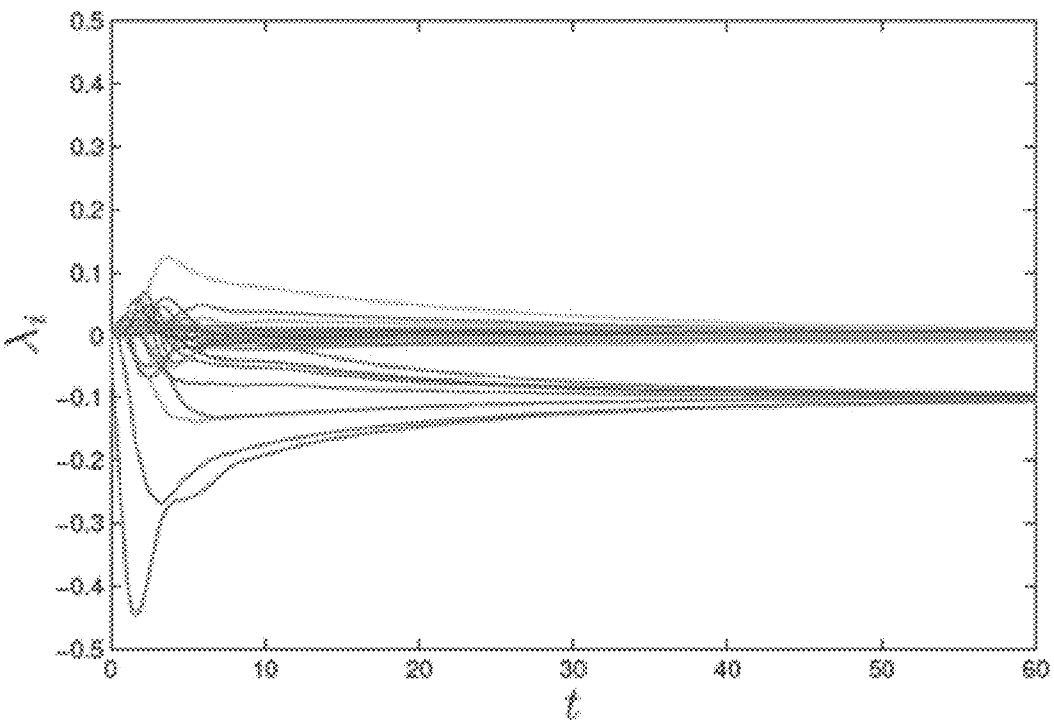

FIG. 15A

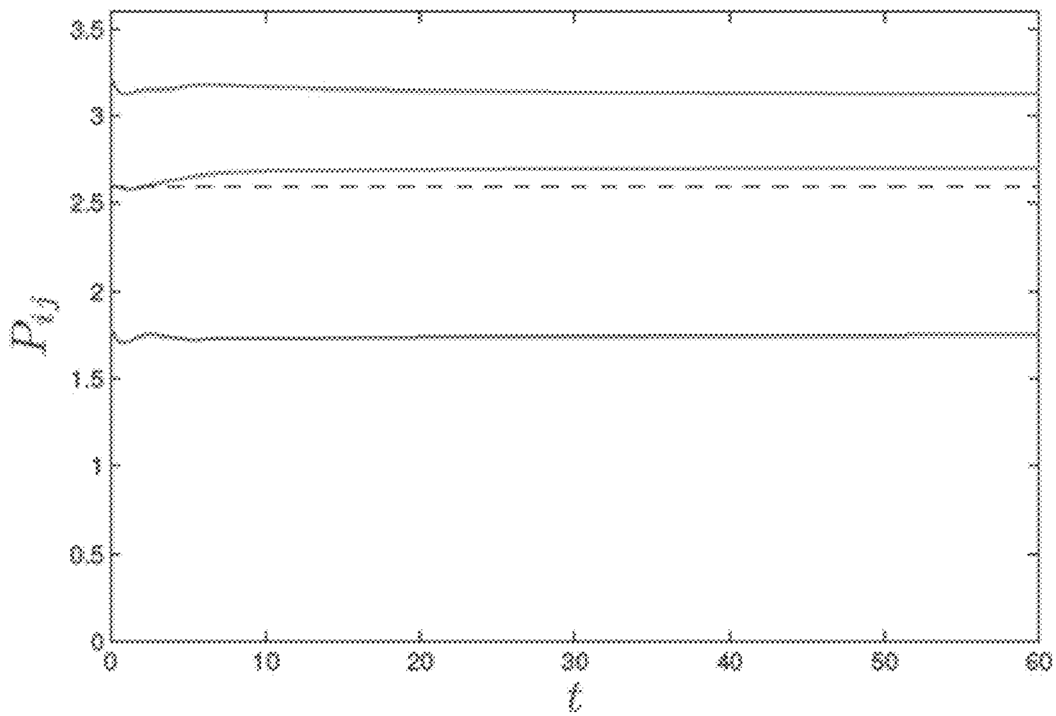

FIG. 15B

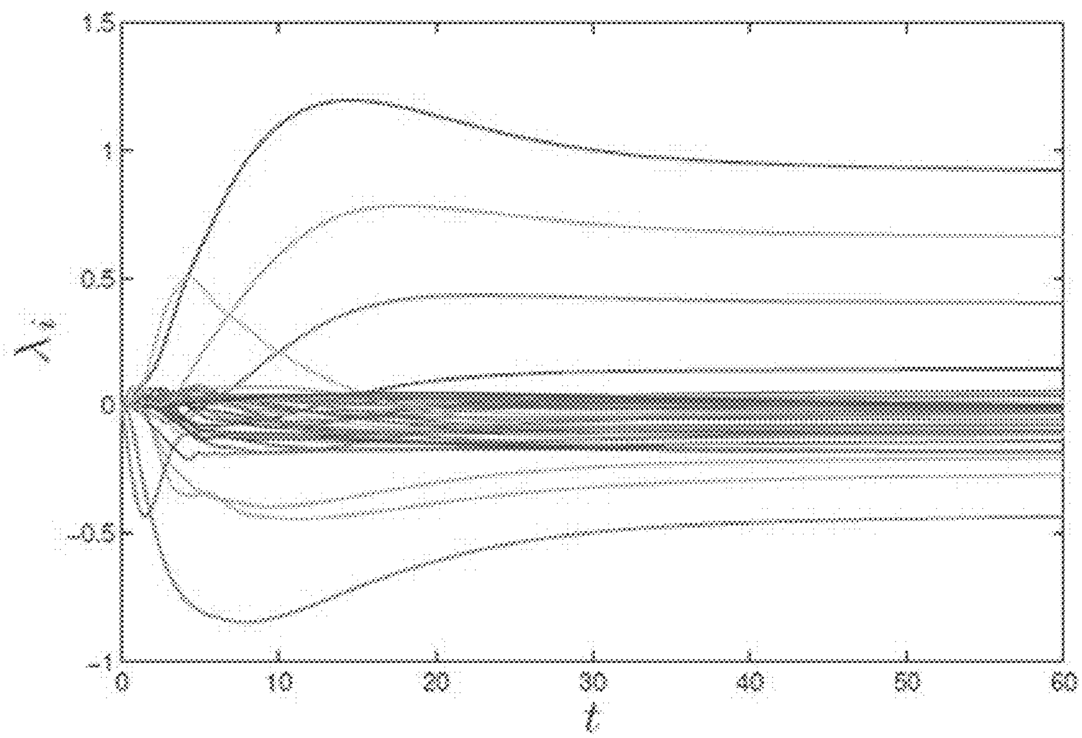

FIG. 16A

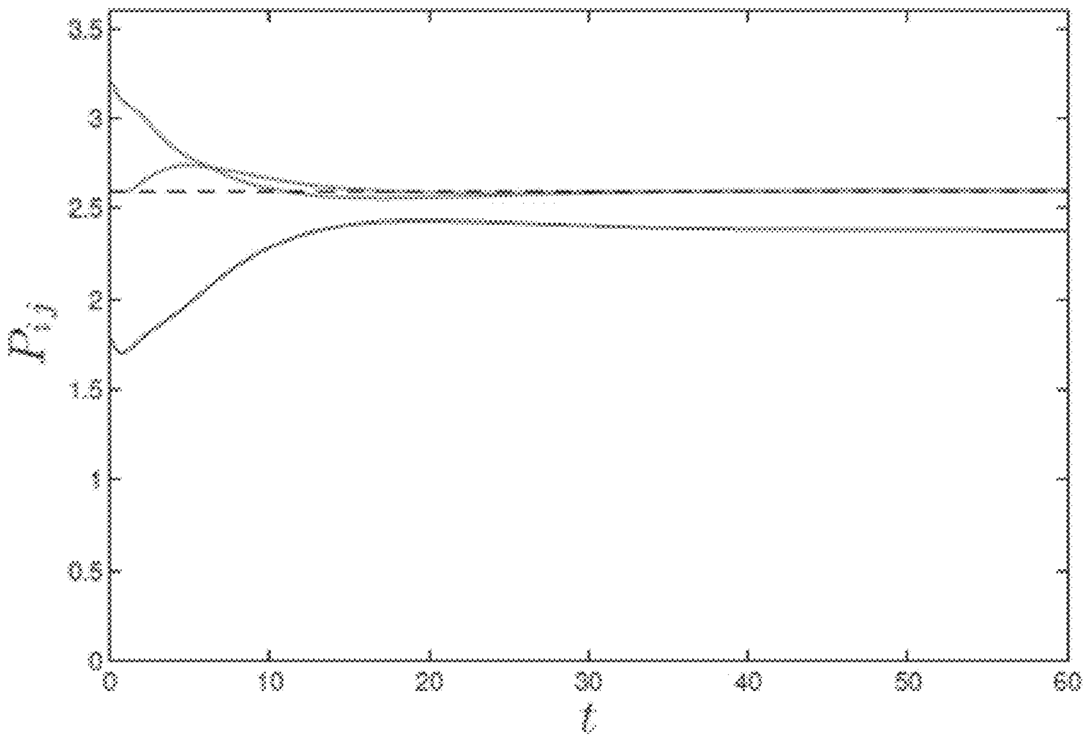

FIG. 16B

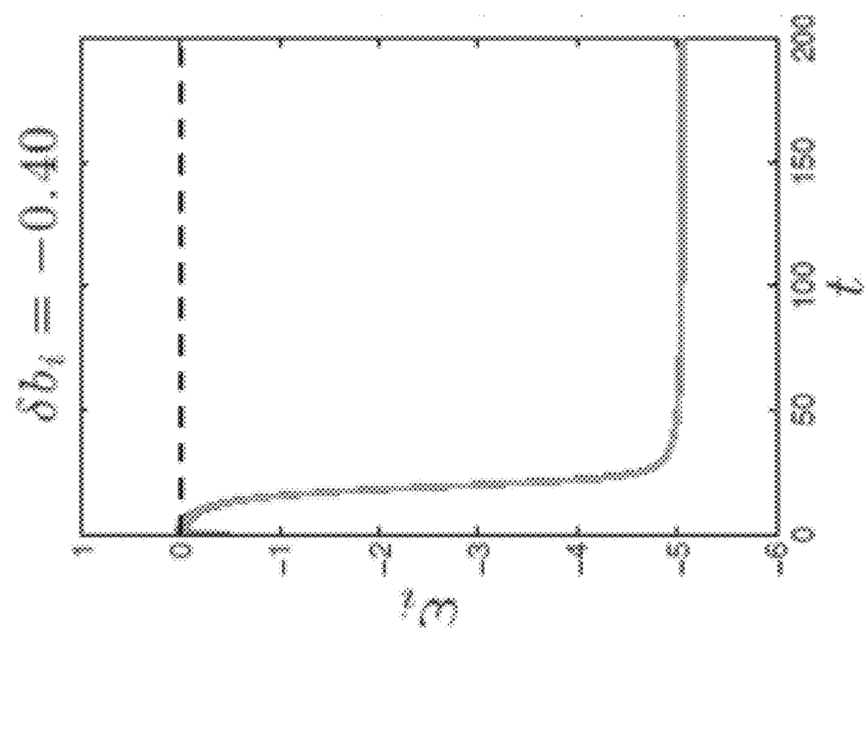

FIG. 17A

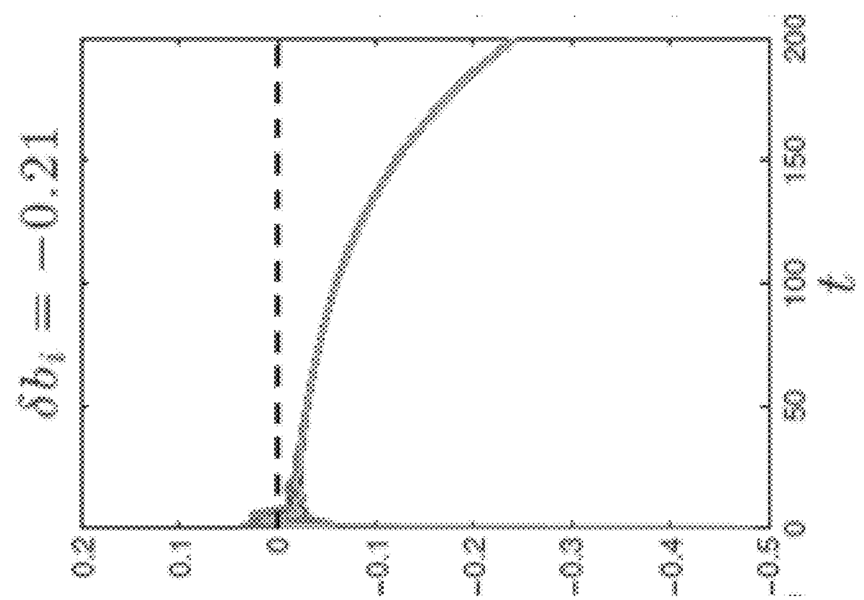

FIG. 17B

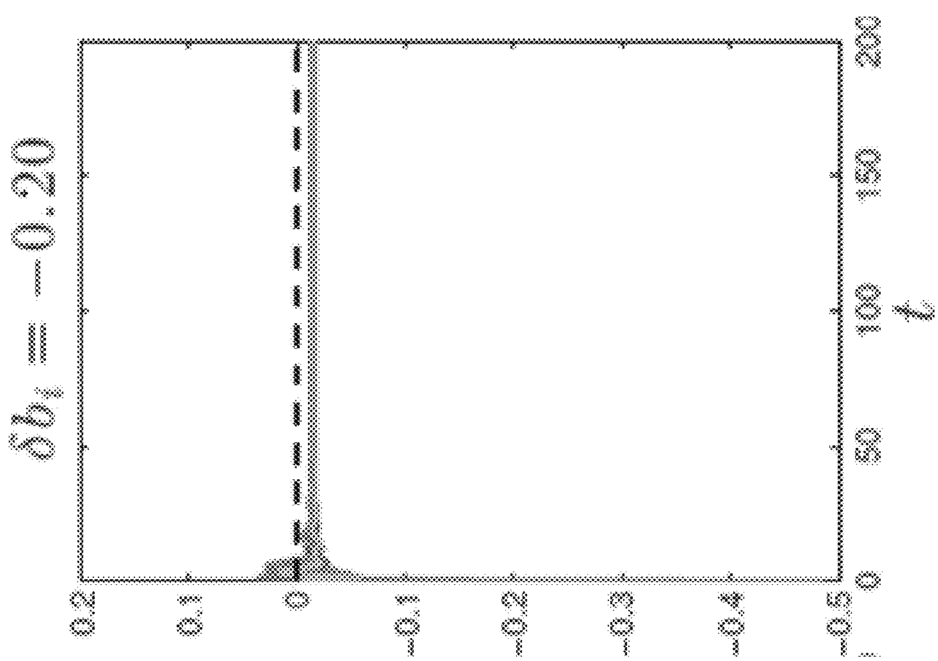

FIG. 17C

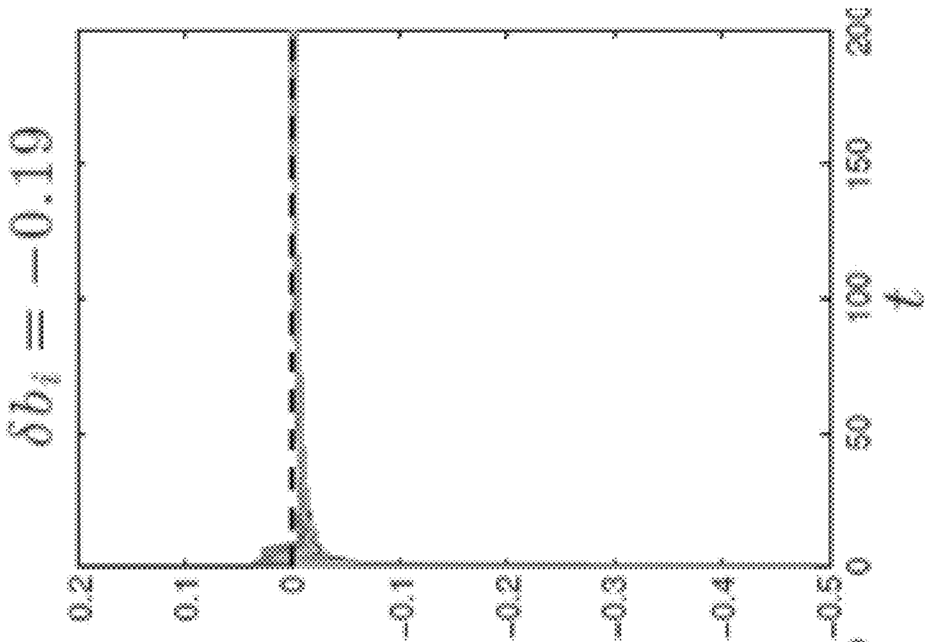

FIG. 17D

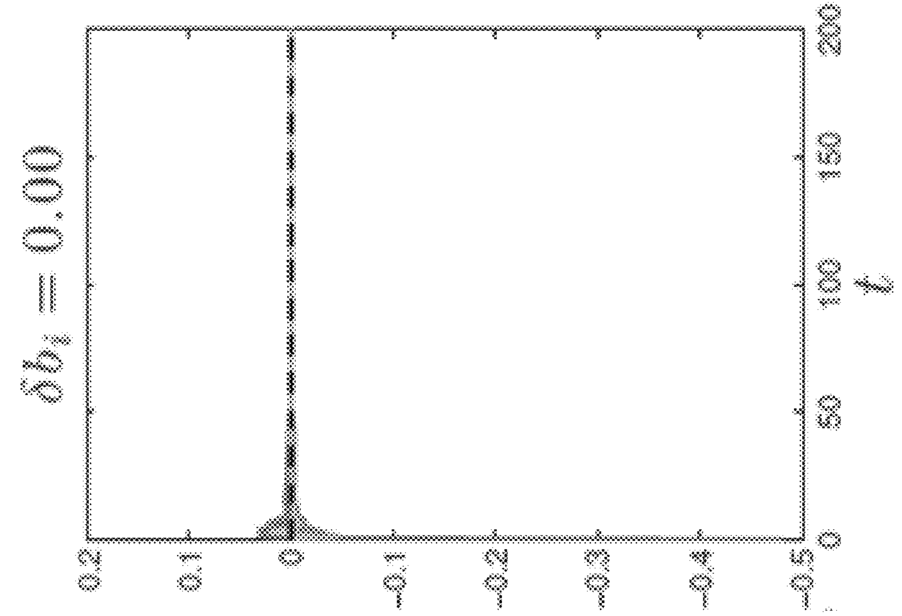

FIG. 17E

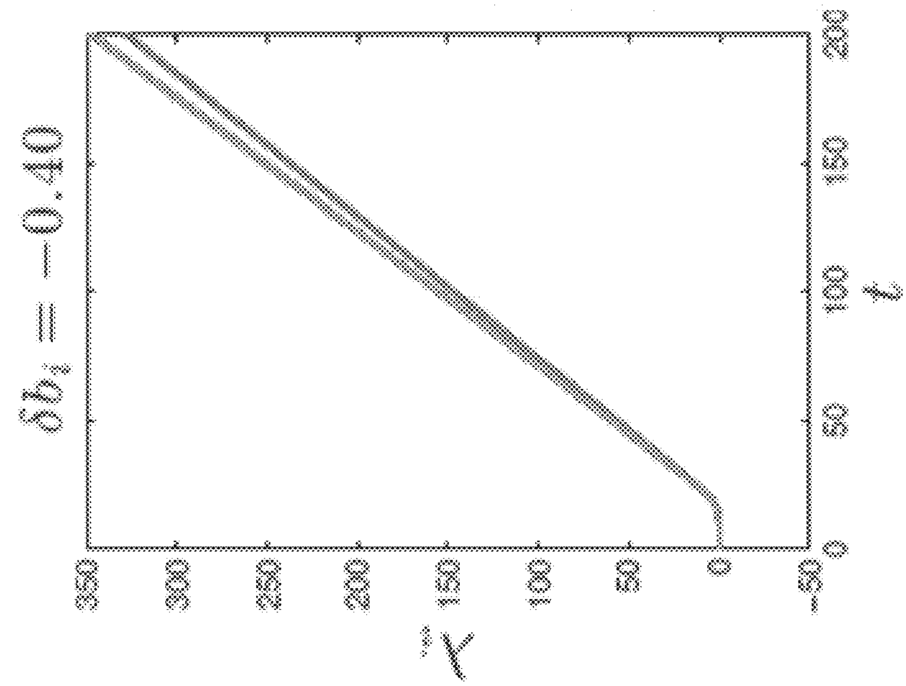

FIG. 18A

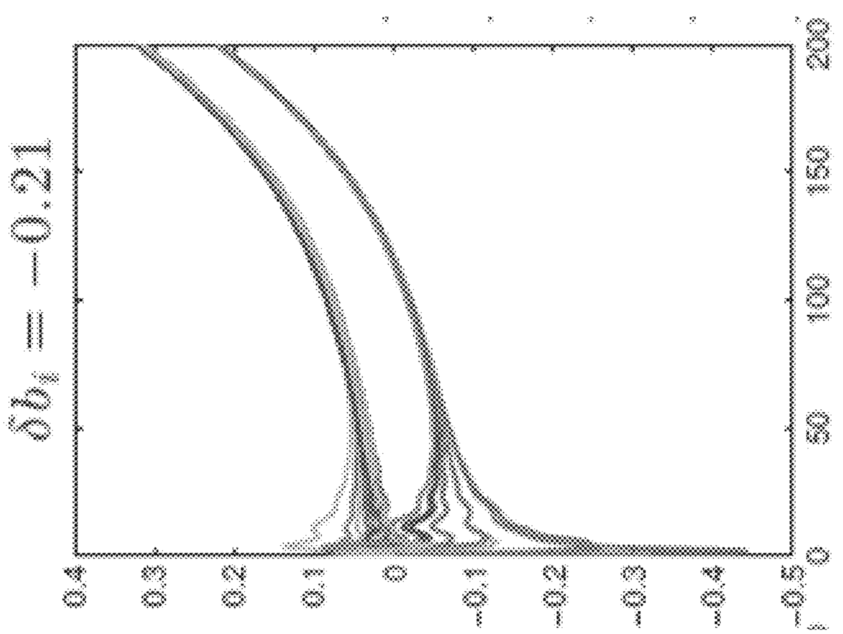

FIG. 18B

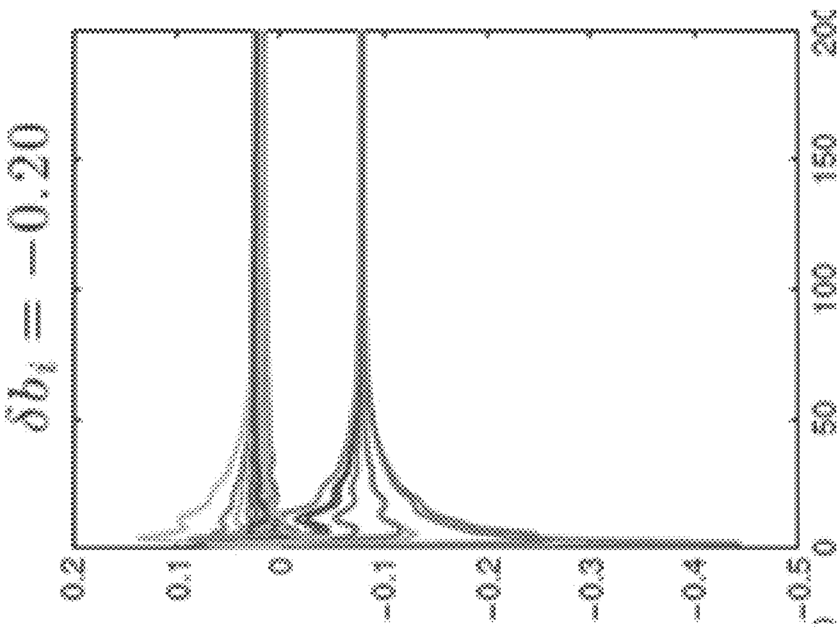

FIG. 18C

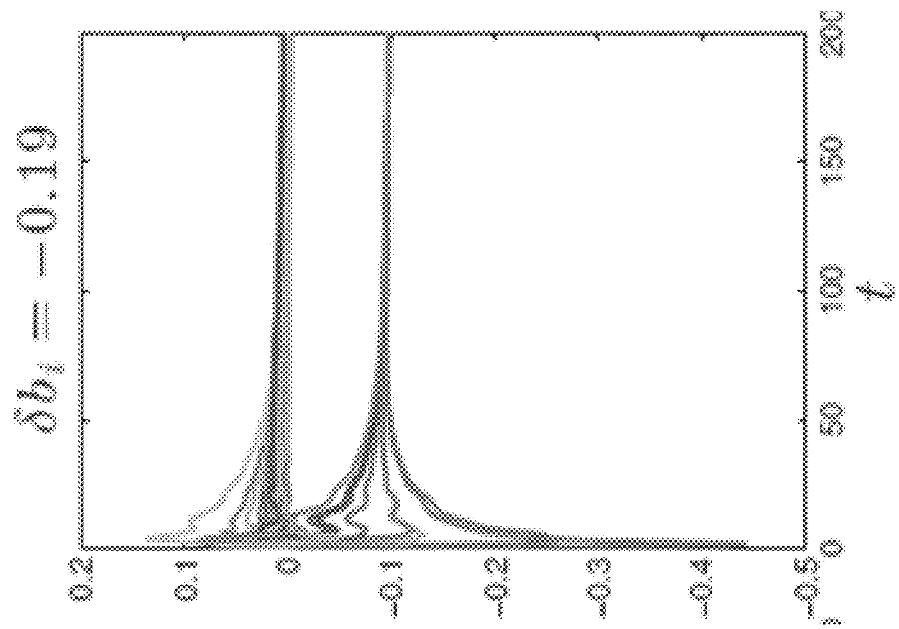

FIG. 18D

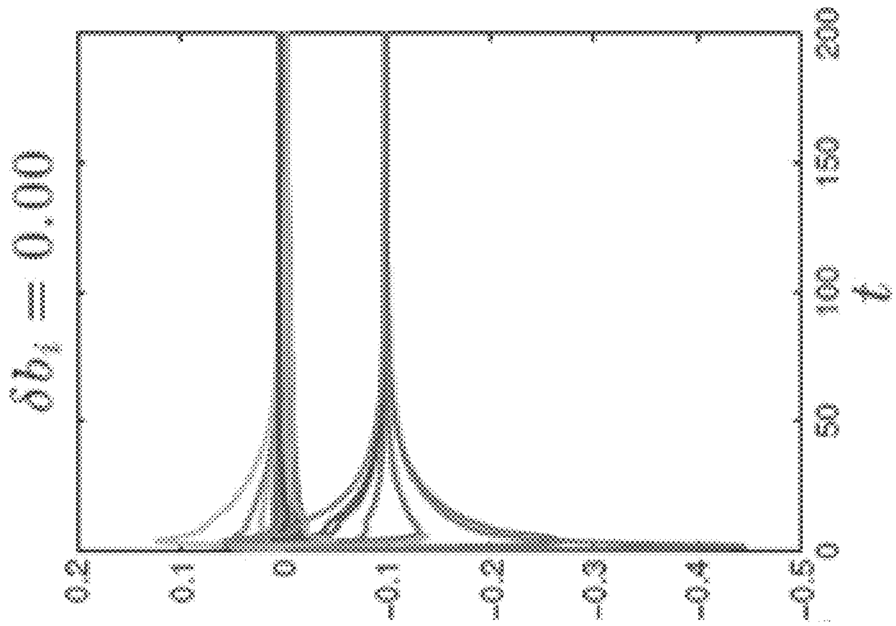

FIG. 18E

DYNAMIC FREQUENCY CONTROL IN POWER NETWORKS

CROSS-REFERENCE TO RELATED APPLICATIONS

[0001] The present invention claims priority to U.S. Provisional Patent Application Ser. No. 62/022,861 entitled "Load-Side Frequency Control in Power Systems" to Zhao et al., filed Jul. 10, 2014. The disclosure of U.S. Provisional Patent Application Ser. No. 62/022,861 is herein incorporated by reference in its entirety.

STATEMENT OF FEDERALLY SPONSORED RESEARCH

[0002] This invention was made with government support under DE-AR0000226 awarded by the U.S. Department of Energy and CNS0911041 awarded by the National Science Foundation. The government has certain rights in the invention.

FIELD OF THE INVENTION

[0003] The present invention generally relates to optimal frequency control and more specifically relates to load side processes for solving for optimal frequency control.

BACKGROUND

[0004] An incredible amount of infrastructure is relied upon to transport electricity from power stations, where the majority of electricity is currently generated, to individual homes. Power stations can generate electricity in a number of ways including using fossil fuels or using renewable sources of energy such as solar, wind, and hydroelectric sources. Once electricity is generated it travels along transmission lines to substations. Substations typically do not generate electricity, but can change the voltage level of the electricity as well as provide protection to other grid infrastructure during faults and outages. From here, the electricity travels over distribution lines to bring electricity to individual homes. The infrastructure used to transport electricity through the power grid can be viewed as a graph comprised of nodes and lines. The power stations, substations, and any end user can be considered nodes within the graph. Transmission and distribution lines connecting these nodes can be represented by lines.

[0005] Distributed power generation, electricity generation at the point where it is consumed, is on the rise with the increased use of residential solar panels and is fundamentally changing the path electricity takes to many users' homes. The term "smart grid" describes a new approach to power distribution which leverages advanced technology to track and manage the distribution of electricity. A smart grid applies upgrades to existing power grid infrastructure including the addition of more renewable energy sources, advanced smart meters that digitally record power usage in real time, and bidirectional energy flow that enables the generation and storage of energy in additional locations along the electrical grid.

SUMMARY OF THE INVENTION

[0006] Node controllers in power distribution networks in accordance with embodiments of the invention enable dynamic frequency control. One embodiment includes a node controller comprising a network interface a processor; and a memory containing a frequency control application; and a plurality of node operating parameters describing the operating parameters of a node, where the node is selected from a group consisting of at least one generator node in a power distribution network wherein the processor is configured by the frequency control application to calculate a plurality of updated node operating parameters using a distributed process to determine the updated node operating parameter using the node operating parameters, where the distributed process controls network frequency in the power distribution network; and adjust the node operating parameters.

[0007] In a further embodiment, the node operating parameters include a node frequency.

[0008] In another embodiment, the node operating parameters include generator node parameters.

[0009] In a still further embodiment, the node operating parameters include a bounded control variable.

[0010] In further additional embodiments, to calculate a plurality of updated node operating parameters using a distributed process processor using the following expression:

$$p_j^c(\omega_j) = [(c_j')^{-1}(-\omega_j)]_{\underline{p}_j}^{\overline{p}_j} \quad j \in \mathcal{G}$$

where p^c is a frequency control parameter, ω is a frequency, c is a cost or disutility function, $\underline{p}_j$ and $\overline{p}_j$ are bounds on the frequency control parameter, j is the node, and $\mathcal{G}$ is the at least one generator node.

[0011] In still another embodiment, a node controller comprising: a network interface; a processor; and a memory containing: a frequency control application; and a plurality of node operating parameters describing the operating parameters of a node, where the node is selected from a group consisting of at least one load node in a power distribution network; wherein the processor is configured by the frequency control application to: calculate a plurality of updated node operating parameters using a distributed process to determine the updated node operating parameter using the node operating parameters, where the distributed process controls network frequency in the power distribution network; and adjust the node operating parameters.

[0012] In a yet further embodiment, the node operating parameters include a node frequency.

[0013] In a still yet further embodiment, the node operating parameters include lode node parameters.

[0014] In another embodiment, the node operating parameters include a bounded control variable.

[0015] In yet another embodiment includes to calculate a plurality of updated node operating parameters using a distributed process is evaluated by the processor using the following expression:

$$p_j(\omega_j) = [(c_j')^{-1}(-\omega_j)]_{\underline{p}_j}^{\overline{p}_j} \quad j \in \mathcal{L}$$

where p is a frequency control parameter, ω is a frequency, c is a cost or disutility function, $\underline{p}_j$ and $\overline{p}_j$ are bounds on the frequency control parameter, j is the node, and $\mathcal{L}$ is the at least one load node.

[0016] In a further embodiment again includes adjusting the node operating parameters further comprises constraining the node operating parameters within thermal limits.

[0017] In another embodiment again includes a power distribution network, comprising one or more centralized computing systems; a communications network; a plurality of generator node controllers, where each generator node controller in the plurality of generator node controllers contains: a generator network interface; a generator node processor; and a generator memory containing: a frequency control application; and a plurality of generator node operating parameters describing the operating parameters of a generator node in a power distribution network; where the generator node processor is configured by the frequency control application to: calculate a plurality of updated generator node operating parameters using a distributed process to determine the updated generator node operating parameter using the generator node operating parameters, where the distributed process controls network frequency in the power distribution network; and adjust the generator node operating parameters; and a plurality of load node controllers, where each load node controller in the plurality of generator node controllers contains: a load network interface; a load node processor; and a load memory containing: the frequency control application; and a plurality of load node operating parameters describing the operating parameters of a load node in the power distribution network; where the load node processor is configured by the frequency control application to: calculate a plurality of updated load node operating parameters using the distributed process to determine the updated load node operating parameter using the load node operating parameters, where the distributed process controls network frequency in the power distribution network; and adjust the load node operating parameters.

[0018] In a still further embodiment again, the generator node operating parameters include a node frequency.

[0019] In still yet another embodiment, the load node operating parameters include a node frequency.

[0020] In a still further embodiment again includes the generator node operating parameters include a bounded control variable.

[0021] In still another embodiment again, the load node operating parameters include a bounded control variable.

[0022] In a further additional embodiment, to calculate a plurality of updated generator node operating parameters using a distributed process is evaluated by the processor using the following expression:

$$p_j^c(\omega_j) = [(c_j')^{-1}(-\omega_j)]_{\underline{p}_j}^{\overline{p}_j} \quad j \in \mathcal{G}$$

where p^c is a frequency control parameter, ω is a frequency, c is a cost or disutility function, $\underline{p}_j$ and $\overline{p}_j$ are bounds on the frequency control parameter, j is the node, and $\mathcal{G}$ is the at least one generator node.

[0023] In another additional embodiment, to calculate a plurality of updated load node operating parameters using the distributed process is evaluated by the processor using the following expression:

$$p_j(\omega_j) = [(c_j')^{-1}(-\omega_j)]_{\underline{p}_j}^{\overline{p}_j} \quad j \in \mathcal{L}$$

where p is a frequency control parameter, ω is a frequency, c is a cost or disutility function, $\underline{p}_j$ and $\overline{p}_j$ are bounds on the frequency control parameter, j is the node, and $\mathcal{L}$ is the at least one load node.

BRIEF DESCRIPTION OF THE DRAWINGS

[0024] FIG. **1** is a diagram conceptually illustrating a power distribution network in accordance with an embodiment of the invention.

[0025] FIG. **2** is a diagram conceptually illustrating nodes utilizing node controllers connected to a communications network in accordance with an embodiment of the invention.

[0026] FIG. **3** is a block diagram illustrating a node controller for optimum frequency control in accordance with an embodiment of the invention.

[0027] FIG. **4** is a flow chart illustrating a process to solve for optimal frequency control in a power distribution network in accordance with an embodiment of the invention.

[0028] FIG. **5** is a flow chart illustrating a process to adjust generator and load parameters in accordance with an embodiment of the invention.

[0029] FIG. **6** is a diagram illustrating an IEEE New England test system for simulations in accordance with an embodiment of the invention.

[0030] FIG. **7** is a diagram illustrating generator frequencies in a simulated optimal frequency control processes in accordance with an embodiment of the invention.

[0031] FIG. **8** is a block diagram illustrating a node controller for optimal load control in accordance with an embodiment of the invention.

[0032] FIG. **9** is a flow chart illustrating a process to solve for optimal load control in a power distribution network in accordance with an embodiment of the invention.

[0033] FIG. **10** is a flow chart illustrating a process to adjust an aggregate controllable load in accordance with an embodiment of the invention.

[0034] FIG. **11** is a diagram illustrating an IEEE 39 bus system for simulations in accordance with an embodiment of the invention.

[0035] FIGS. **12**A-**12**B are diagrams illustrating a cost or disutility function and an aggregate controllable load respectively in accordance with an embodiment of the invention.

[0036] FIGS. **13**A-**13**C are diagrams illustrating the evolution of node frequencies in simulated area 1 in accordance with an embodiment of the invention.

[0037] FIGS. **14**A-**14**C are diagrams illustrating the evolution in node frequencies in simulated area 2 in accordance with an embodiment of the invention.

[0038] FIGS. **15**A-**15**B are diagrams illustrating LMPs and inter area line flows respectively without thermal limits in optimal load control simulations in accordance with an embodiment of the invention.

[0039] FIGS. **16**A-**16**B are diagrams illustrating LMPs and inter area line flows respectively with thermal limits in optimal load control simulations in accordance with an embodiment of the invention.

[0040] FIGS. **17**A-**17**E are diagrams illustrating node frequency evolution for optimal load control simulations in accordance with an embodiment of the invention.

[0041] FIGS. **18**A-**18**E are diagrams illustrating location marginal prices evolution for optimal load control simulations in accordance with an embodiment of the invention.

DETAILED DESCRIPTION

[0042] Turning now to the drawings, systems and methods for dynamic load control in power networks in accordance with embodiments of the invention are illustrated. Power frequency control maintains frequency in a power distribution network as power supply and demand change. Frequency control traditionally occurs on the generator side of the power distribution network, but it can also occur on the load side of the network. A power distribution network can be partitioned into generator side and load side portions based on supply or demand roles.

[0043] An optimization problem can be utilized to increase the performance of the network with respect to particular goals. The optimal frequency control (OFC) problem typically seeks to minimize total generation cost, user disutility, and/or other operational constraints, and will be the focus of SECTION 1 below. In several embodiments, the OFC problem can maintain power balance across an entire power distribution network by controlling frequency on the generation side and/or the load side.

[0044] The OFC problem can be solved when equilibrium points are found. In various embodiments, an approach to solving for these equilibrium points is through the use of a primal-dual algorithm approach. An extension of this approach is to use partial primal-dual algorithms. Primal-dual algorithms can lend nicely to distributed solutions and these distributed solutions can then be utilized to develop control processes for components of the power distribution networks. Specifically, distributed solutions frequently do not require explicit communication between portions of the network and/or knowledge of overall system parameters. In many embodiments, generator side and load side frequency control occur simultaneously to solve for OFC. Generating power in a power distribution network can be a complicated process. In various embodiments, models used for solving the OFC problem can include power generation with the addition of turbines and governors.

[0045] An alternative optimization problem, the optimal load control (OLC) problem will be the focus of SECTION 2 further below. The OLC problem seeks to minimize aggregate disutility. In many embodiments, the OLC problem can balance power across an entire network by controlling aggregate load on the load side. Similar to SECTION 1, a primal-dual algorithm can be used, which lends itself to a distributed solution. In various embodiments it can be useful to add additional constraints to an increasingly complicated model, for example (but not limited to) to constrain the power line flow within thermal limits.

Frequency in Power Networks

[0046] A power distribution network in accordance with an embodiment of the invention is shown in FIG. **1**. Electricity is generated in power generator **102**. Power transmission lines **104** can transmit electricity between the power generator and power substation **106**. Power substation **106** additionally can connect to large storage battery **108**, which temporarily stores electricity, as well as power distribution lines **110**. The power distribution lines **110** can transmit electricity from the power substation to homes **112**. The homes can include solar panels **114**, a house battery **116**, and/or an electric car **118**. In a number of embodiments, processes are utilized that achieve OFC and/or OLC in power distribution networks.

[0047] The power generator **102** can represent a power source including those using fossil fuels, nuclear, solar, wind, and/or hydroelectric power. In various embodiments, multiple power generators **102** may be present. Substation **106** changes the voltage of the electricity for more efficient power distribution. Solar panels **114** are distributed power generation sources, and can generate power to supply the home as well as generate additional power for the power grid. House battery **116** can store excess electricity from the solar panels to power the home when solar energy is unavailable, or store electricity from the power grid to use at a later time. Substations **106**, large storage batteries **108**, homes **112**, solar panels **114**, house batteries **116**, and electric cars **118** can all be considered to be nodes within the power distribution network and the distribution lines **110** can be considered to be lines within the power distribution network. Additional items that draw electricity may also be located within house **112** including (but not limited to) washing machines, dryers, refrigerators, hair dryers, computers, lamps, and/or televisions. In some embodiments these additional items can also be nodes. In combination, nodes and lines form a power distribution network.

[0048] Nodes within the power distribution network may have different roles. Nodes that are creating power (such as power generator **102** or solar panels **112**) can be generator nodes on the generator side of the network, and nodes which consume power (such as electric cars **118** or additional items connected to the network within a house) can be load nodes on the load side of the network. In many embodiments, OFC and/or OLC can be attained through generator side frequency control, load side frequency control, and/or a combination of generator and load side frequency control.

[0049] In many embodiments, node controllers are located at nodes throughout the network to control the operating parameters of different nodes to achieve OFC and/or OLC. Connected nodes can be nodes within the power distribution network that are connected by distribution and/or transmission lines and can be controlled by a node controller. The type of control utilized can depend on the specifics of the network and may include distributed, centralized, and/or hybrid power control. Although many different systems are described above with reference to FIG. **1**, any of a variety of power distribution networks including node controllers may be utilized to perform power distribution as appropriate to the requirements of specific applications in accordance with embodiments of the invention. Nodes utilizing node controllers connected to a communication network in accordance with various embodiments of the invention are discussed further below.

Node Controller Architectures

[0050] Nodes utilizing node controllers connected to a communication network in accordance with an embodiment of the invention are shown in FIG. **2**. Nodes **202** can connect to communication network **204** using a wired and/or wireless connection **206**. In some embodiments the power distribution network can act in place of the communication network. The communication network may also be connected to one or more centralized computer systems **208** to monitor calculations made by or to send instructions to multiple node controllers to, for example, control power distribution in the network at a global level. Additionally, in many embodiments a database management system **210** can be connected to the network to track node data which, for example, may be used to historically track power usage and/or frequencies at various locations over time. Although various system configurations are described above with reference to FIG. **2**, any number of systems can be utilized to achieve control of nodes within a power distribution network as appropriate to the requirements of specific applications in accordance with embodiments of the invention. Node controllers for OFC in accordance with various embodiments of the invention are discussed further below.

Section 1

Node Controllers for Optimal Frequency Control

[0051] A node controller in accordance with an embodiment of the invention is shown in FIG. **3**. In various embodiments, node controller **300** can perform calculations in a distributed manner at a node in a power distribution network. The node controller includes at least one processor **302**, an I/O interface **304**, and memory **306**. The at least one processor **302**, when configured by software stored in memory, can perform calculations on and make changes to data passing through the I/O interface as well as to data stored in memory. In many embodiments, the memory **306** includes software including frequency control application **308** as well as node frequency **310**, node operating parameters **312**, generator node parameters **314**, and load node parameters **316**. A node can measure node frequency through the I/O interface and/or receive this value from a centralized computer. The frequency control application **308** will be discussed in greater detail below and can enable the node to perform calculations to solve for optimal frequency control in a distributed manner. These distributed calculations can be performed such that only node operating parameters **312** and node frequency **310** need to be known by the node, and no communication with other nodes or knowledge of system parameters are required.

[0052] Node operating parameters will be discussed in detail below but may include (but are not limited to) a cost function, a utility function, and/or bounds of control variables. Distributed calculations will generate generator node parameters **314** in the case of a generator node and load node parameters **316** in the case of a load node. In various embodiments, the same node controller can be used for both generator and load nodes. It should be readily apparent node controller **300** can be adapted to generator node or load node specific applications, or a hybrid controller that can switch between specific node types as requirements of specific applications require. Although a number of different node controller implementations are discussed above with reference to FIG. **3**, any of a variety of computing systems can be utilized to control a node within a power distribution system as appropriate to the requirements of specific applications in accordance with various embodiments of the invention. Graph representations of a power distribution network in accordance with several embodiments of the invention are discussed further below.

Power Network Graph Representations

[0053] In various embodiments, the following graph representation is utilized to represent at least a portion of a power distribution network. Let $\mathbb{R}$ denote the set of real numbers. For a set $\mathcal{N}$, let $\mathcal{N}$ denote its cardinality. A variable without a subscript usually denotes a vector with appropriate components, e.g., $\omega=(\omega_j,\ j\in\mathcal{N})\in\mathbb{R}^{|\mathcal{N}|}$. For a, $b\in\mathbb{R}$, $a\le b$, the expression $[\bullet]_a^b$ denotes max $\{\min(\{\bullet, b\}, a\}$. For a matrix A, A^T can denote its transpose. For a square matrix A, the expression $A\succ 0$ indicates it is positive definite and $A\prec 0$ indicates the matrix is negative definite. For a signal $\omega(t)$ of time t, let ω denote its time derivative $d\omega/dt$.

[0054] The classical structure preserving model can be combined with generator speed governor and turbine models. The power network is modeled as a graph $(\mathcal{N}, \epsilon)$ where $\mathcal{N}=\{1, \ldots, |\mathcal{N}|\}$ is the set of nodes (buses) and $\epsilon\subseteq\mathcal{N}\times\mathcal{N}$ is the set of lines connecting those nodes (buses). The line connecting nodes (buses) i, $j\in\mathcal{N}$ can be denoted by (i, j), and in several embodiments it can be assumed that (N, ϵ) is directed, with an arbitrary orientation, so that if $(i, j)\in\epsilon$ then $(j, i)\notin\epsilon$. "$i:i\rightarrow j$" and "$k:j\rightarrow k$" can respectively be used to denote the set of nodes (buses) i that are predecessors of node (bus) j and the set of nodes (buses) k that are successors of node (bus) j. In many embodiments, it can be assumed without loss of generality that (N, ϵ) is connected, and the following assumptions can be utilized: lines $(i, j)\in\epsilon$ are lossless and characterized by their reactances x_{ij}, voltage magnitudes $|V_j|$ of nodes (buses) $j\in\mathcal{N}$ are constants, and reactive power injections on nodes (buses and reactive power flows on lines are not considered.

[0055] A subset $\mathcal{G}\subset\mathcal{N}$ of the nodes (buses) are fictitious nodes (buses) representing the internal of generators. Hence, the set $\mathcal{G}$ can be called the set of generators and the set $\mathcal{L}=\mathcal{N}\setminus\mathcal{G}$ can be the set of load nodes (buses). All the nodes (buses) in $\mathcal{L}$ can be called load nodes (buses) without distinguishing between generator nodes (buses) (nodes connected directly to generators) and actual load nodes (buses), since they can be treated in the same way mathematically. The nodes (buses) can be labeled so that $\mathcal{G}=\{1, \ldots, |\mathcal{G}|\}$ and $\mathcal{L}=\{|\mathcal{G}|+1, \ldots, |\mathcal{N}|\}$.

[0056] The voltage phase angle of node (bus) $j\in\mathcal{N}$, with respect to the rotating framework of nominal frequency $\omega_0=120\pi$ rad/s, can be denoted by θ_j. The frequency deviation of node (bus) j from the nominal frequency ω_0 can be denoted by ω_j. Hence

$$\dot{\theta}_j=\omega_j\, j\in\mathcal{N}. \tag{1}$$

The system dynamics are described by the swing equations

$$M_j\dot{\omega}_j=-D_j\omega_j+p_j-F_j(\theta) j\in\mathcal{N} \tag{2}$$

where $M_j>0$ for $j\in\mathcal{G}$ are moments of inertia of generators and $M_j=0$ for $j\in\mathcal{L}$, and $D_j>0$ for all $j\in\mathcal{N}$ are (for $j\in\mathcal{G}$) the damping coefficients of generators or (for $j\in\mathcal{L}$) the coefficients of linear frequency dependent loads, e.g., induction motors. The variable p_j denotes the real power injection to node (bus) j, which is the mechanic power injection to generator if $j\in\mathcal{G}$, and is the negative of real power load if $j\in\mathcal{L}$. The net real power flow out of node (bus) j is

$$F_j(\theta):=\sum_{k:j\rightarrow k} Y_{jk}\sin(\theta_j-\theta_k)-\sum_{i:i\rightarrow j} Y_{ij}\sin(\theta_i-\theta_j)\quad j\in\mathcal{N} \tag{3}$$

where

$$Y_{jk} := \frac{|V_j||V_k|}{x_{jk}}$$

are the maximum real power flows on lines $(j, k) \in \epsilon$.

[0057] In various embodiments, a system of governor and turbine can be associated with a generator $j \in \mathcal{G}$, and their dynamics can be described by

$$\dot{a}_j = -\frac{1}{\tau_{g,j}} a_j + \frac{1}{\tau_{g,j}} p_j^c \quad j \in \mathcal{G} \tag{4}$$

$$\dot{p}_j = -\frac{1}{\tau_{b,j}} p_j + \frac{1}{\tau_{b,j}} a_j \quad j \in \mathcal{G} \tag{5}$$

where a_j is the valve position of the turbine, p_j^c is the control command to the generator, and p_j, as introduced above, is the mechanic power injection to the generator. The time constants $\tau_{g,j}$ and $\tau_{b,j}$ characterize respectively the time-delay in governor action and the approximated fluid dynamics in the turbine. Traditionally, there is a frequency feedback term

$$-\frac{1}{R_j}\omega_j$$

added to the right-handside of (4), known as the frequency droop control. Here this term is merged into p_j^c to allow for a general form of frequency feedback control.

[0058] Equations (1)-(5) specify a dynamical system with state variables $(\theta, \omega, a_{\mathcal{G}}, p_{\mathcal{G}})$ where

$$\theta := \{\theta_1, \ldots, \theta_{|\mathcal{N}|}\}, \quad \omega := \{\omega_1, \ldots, \omega_{|\mathcal{N}|}\}$$

$$a_{\mathcal{G}} := \{a_1, \ldots, a_{|\mathcal{G}|}\}, \quad p_{\mathcal{G}} := \{p_1, \ldots, p_{|\mathcal{G}|}\}$$

and input variables $(p_{\mathcal{G}}^c, p_{\mathcal{L}})$ where

$$p_{\mathcal{G}}^c := \{p_1^c, \ldots, p_{|\mathcal{G}|}^c\}, \quad p_{\mathcal{L}} := \{p_{|\mathcal{G}+1|}, \ldots, p_{|\mathcal{N}|}\}.$$

$(p_{\mathcal{G}}^c, p_{\mathcal{L}})$ are feedback control to be designed based on local measurements of frequency deviations, i.e., $(p_{\mathcal{G}}^c(\omega), p_{\mathcal{L}}(\omega))$. Parameters $\underline{p} \le \overline{p}_j$ specify the bounds of the control variables, i.e., $\underline{p}_j \le p_j^c(\omega) \le \overline{p}_j$ for $j \in \mathcal{G}$, and $\underline{p}_j \le p_j(\omega) \le \overline{p}_j$ for $j \in \mathcal{L}$. Note that if $\underline{p}_j = \overline{p}_j$ then they specify a constant, uncontrollable input on node (bus) j. This can create a closed-loop dynamical system, and equilibrium points for this system will be described below.

Equilibrium Points

[0059] Definition 1. An equilibrium point of the system (1)-(5) with control $(p_{\mathcal{G}}^c(\omega), p_{\mathcal{L}}(\omega))$, (referred to as a closed-loop equilibrium for short), is $(\theta^*, \omega, a_{\mathcal{G}}^*, p_{\mathcal{G}}^*, p_{\mathcal{G}}^{c,*}, p_{\mathcal{L}}^*)$, where θ^* is a vector function of time and $(\omega^*, a_{\mathcal{G}}^*, p_{\mathcal{G}}^*, p_{\mathcal{G}}^{c,*}, p_{\mathcal{L}}^*)$ are vectors of real numbers, such that

$$p_{\mathcal{G}}^{c,*} = p_{\mathcal{G}}^c(\omega^*), \quad p_{\mathcal{L}}^* = p_{\mathcal{L}}(\omega^*) \tag{6}$$

$$d\theta^*_j/dt = \omega^*_j \; j \in \mathcal{N} \tag{7}$$

$$\omega^*_i = \omega^*_j = \omega^* \; i,j \in \mathcal{N} \tag{8}$$

$$-D_j\omega^*_j + p^*_j - F_j(\theta^*) = 0 \; j \in \mathcal{N} \tag{9}$$

$$p^*_j = a^*_j = p_j^{c,*} \; j \in \mathcal{G}. \tag{10}$$

[0060] Notation can be abused by using ω^* to denote both the vector $(\omega^*_1, \ldots, \omega^*_{|\mathcal{N}|})$ and the common value of its components. Its meaning should be clear from the context.

[0061] In the definition above, (8) ensures constant $F(\theta^*)$ at equilibrium points by (3), and (9)(10) are obtained by letting right-hand-sides of (2)(4)(5) be zero. From (8), at any equilibrium point, all the nodes (buses) are synchronized to the same frequency. The system typically has multiple equilibrium points as will be explained in detail below. An equilibrium point can also be written as $(\theta^*, \omega^*, a_{\mathcal{G}}^*, p_{\mathcal{G}}^{c,*}, p^*)$ where $p^* := (p_{\mathcal{G}}^*, p_{\mathcal{L}}^*)$, when state variables $p_{\mathcal{G}}^*$ and control variables $p_{\mathcal{L}}^*$ do not need to be distinguished.

Decentralized Primary Frequency Control

[0062] An initial point of the dynamical system (1)-(5) corresponds to the state of the system at the time of fault-clearance after a contingency, or the time at which an unscheduled change in power injection occurs during normal operation. In either case, the system trajectory, driven by primary frequency control $(p_{\mathcal{G}}^c(\omega), p_{\mathcal{L}}(\omega))$, converges to a desired equilibrium point. The criteria for desired equilibrium points can be formalized by formulating an optimization problem called optimal frequency control (OFC), and using OFC to guide the design of control processes for various components within a power distribution network.

Optimal Frequency Control Problem

[0063] In several embodiments, the objective in the power distribution network can be to rebalance power after a disturbance at a minimum generation cost and user disutility. This can be formalized by requiring any closed-loop equilibrium (p^*, d^*) to be a solution of the following OFC problem, where $d_j = D_j\omega^*_j$ for $j \in \mathcal{N}$.

$$\min_{p,d} \sum_{j \in \mathcal{N}} \left(c_j(p_j) + \frac{1}{2D_j} d_j^2 \right) \tag{11}$$

$$\text{subject to} \sum_{j \in \mathcal{N}} (p_j - d_j) = 0 \tag{12}$$

$$\underline{p}_j \le p_j \le \overline{p}_j \quad j \in \mathcal{N}. \tag{13}$$

The term $c_j(p_j)$ in objective function (11) is generation cost (if $j \in \mathcal{G}$) or user disutility for participating in load control (if $j \in \mathcal{L}$). For simplicity c_j can be called a cost function for $j \in \mathcal{N}$ even if it may be a user disutility function. The term

$$\frac{1}{2D_j} d_j^2$$

implicitly penalizes frequency deviation on node (bus) j at equilibrium. The constraint (12) can ensure power balance over an entire network, and (13) can be bounds on power injections. These bounds can be determined by control capacities of generators or controllable loads, as well as uncontrollable power injections as an exogenous input.

[0064] In many embodiments, the following assumptions can be utilized:

Condition 1. OFC is feasible. The cost functions c_j are strictly convex and twice continuously differentiable on $(\underline{p}_j, \overline{p}_j)$.

Remark 1. A load $-p_j$ on node (bus) $j \in \mathcal{L}$ results in a user utility $u_j(-p_j)$, and hence the disutility function can be defined as $c_j(p_j) = -u_j(-p_j)$. The user disutility functions or generation cost functions usually satisfy Condition 1, and in many cases are quadratic functions.

Condition 2. For any optimal solution (p^*, d^*) of OFC, the power flow equations

$$F_j(\theta) = p^*_j - d^*_j, j \in \mathcal{N} \tag{14}$$

are feasible, i.e., have at least one solution $\theta^* \in \mathbb{R}^{|\mathcal{N}|}$.

Remark 2. Condition 2 ensures the existence of a closed-loop equilibrium of the dynamical system (1)-(5) with the feedback control described below.

Design of Decentralized Feedback Control

[0065] An overview of a process for solving for optimal frequency control in a power distribution network is illustrated in FIG. **4**. In process **400**, the frequency of each node is measured **402**. Optimal frequency control is achieved **404** for the power network by controlling generator node parameters and load node parameters using the measured node frequency.

[0066] A process for a node to adjust generator node parameters and/or load node parameters is illustrated in FIG. **5**. Referring above to FIG. **3** and FIG. **4**, the process can be similar to parts of process **400** and can be performed by a node controller similar to node controller **300**. Process **500** includes measuring **502** frequency of the node. If the node is a generator node **504**, generator node parameters are calculated **506** using the node frequency and node operating parameters. Generator node parameters are adjusted **508** and the process completes. If the node is not a generator node **504**, and is a load node **510**, load node parameters are calculated **512** using the node frequency and node operating parameters. Load node parameters are adjusted **514** and the process completes. If the load is neither a generator node **504** nor a load node **510**, the process completes. This process will be described in detail below.

[0067] As noted above, OFC can be used to guide controller design. In various embodiments, $(p^c_{\mathcal{G}}(\omega), p_{\mathcal{L}}(\omega))$ can be designed as

$$p^c_j(\omega_j) = [(c'_j)^{-1}(-\omega_j)]^{\overline{p}_j}_{\underline{p}_j} \quad j \in \mathcal{G} \tag{15}$$

$$p_j(\omega_j) = [(c'_j)^{-1}(-\omega_j)]^{\overline{p}_j}_{\underline{p}_j} \quad j \in \mathcal{L}. \tag{16}$$

The function $(c'_j)^{-1}(\bullet)$, which is the inverse function of the derivative of the cost function, is well defined if Condition 1 holds. Note that this control is completely decentralized in that for every generator and load indexed by j, the control decision is a function of frequency deviation ω_j measured at its local node (bus). Only its own cost function c_j and bounds $[\underline{p}_j, \overline{p}_j]$ need to be known. No explicit communication with other generators and loads is required, nor is any knowledge of system parameters. Moreover, the following theorem shows that this design fulfills OFC objectives.

Theorem 1. Suppose Conditions 1 and 2 hold, it can be proven that:

[0068] 1. There is a unique optimal solution of OFC and its dual.

[0069] 2. For the system (1)-(5) with control (48)(48), there exists at least one equilibrium point. Let $(\theta^*, \omega^*, a^*_{\mathcal{G}}, p^{c,*}_{\mathcal{G}}, p^*)$ be any of its equilibrium point(s). Then $(p^*, d^*; \omega^*)$ is the unique optimal solution of OFC and its dual, where $d^*_j = D_j\omega^*$ for $j \in \mathcal{N}$

Optimal Frequency Control Simulations

[0070] The performance of the proposed control can be illustrated through a simulation of the IEEE New England test system shown in FIG. **6**. FIG. **6** illustrates an IEEE New England Test system. This system has 10 generators and 39 nodes (buses), and a total load of about 60 per unit (pu) where 1 pu represents 100 MVA. Compared to the model (2)-(4), the simulation model is more detailed and realistic, with transient generator dynamics, excitation and flux decay dynamics, changes in voltage and reactive power over time, and lossy transmission lines, et cetera. The test system in FIG. **6** is similar to the test system described below with respect to in FIG. **11**.

[0071] The primary frequency control of generator or load j is designed with cost function

$$c_j(p_j) = \frac{R_j}{2}(p_j - p_j^{set})^2,$$

where p_j^{set} is the power injection at the setpoint, an initial equilibrium point solved from static power flow problem. By choosing this cost function, the deviations of power injections from the setpoint can be attempted to be minimized, and have the control

$$p_j = \left[p_j^{set} - \frac{1}{R_j}\omega_j\right]^{\overline{p}_j}_{\underline{p}_j}$$

from (48)(48). Only the load control p_j for $j \in \mathcal{L}$ is written since the generator control p_j^c for $j \in \mathcal{G}$ takes the same form. The following two simulated cases can be considered in which the generators and loads have different control capabilities and hence different $[\underline{p}_j, \overline{p}_j]$:

[0072] 1. All the 10 generators have $[\underline{p}_j, \overline{p}_j] = [p_j^{set}(1-c), p_j^{set}(1+c)]$, and all the loads are uncontrollable;

[0073] 2. Generators 2, 4, 6, 8, 10 (which happen to provide half of the total generation) have the same bounds as in case (1). Generators 1, 3, 5, 7, 9 are uncontrollable, and all the loads have $[\underline{p}_j, \dot{p}_j] = [p_j^{set}(1+c/2), p_j^{set}(1-c/2)]$, if $p_j^{set} \le 0$ for loads $j \in \mathcal{L}$.

Hence simulated cases (1) and (2) have the same total control capacity across the network. Case (1) only has generator control while in case (2) the set of generators and the set of loads each has half of the total control capacity. c=10% can be selected, which implies the total control capacity is about 6 pu. For all $j \in \mathcal{N}$, the feedback gain $1/R_j$ is selected as $25\, p_j^{set}$, which is a typical value in practice meaning a frequency change of 0.04 pu (2.4 Hz) causes the change of power injection from zero all the way to the setpoint. Note that this control is the same as frequency droop control, which implies that indeed frequency droop control implicitly solves an OFC problem with quadratic cost functions used here. However, the simulated controller design can be more flexible by allowing a larger set of cost functions.

[0074] In several embodiments, the simulated system is initially at the setpoint with 60 Hz frequency. At time t=0.5 second, nodes (buses) 4, 15, 16 each makes 1 pu step change in their real power consumptions, causing the frequency to drop. FIG. **7** illustrates the frequencies of all the 10 generators under case (1) only generators are controlled (red) and case (2) both generators and loads are controlled (black). The total control capacities are the same in these two cases. It can be seen in both cases that frequencies of different generators have relatively small differences during transient, and are synchronized towards the new steady-state frequency. Compared with simulated generator-only control, the combined simulated generator-and-load control improves both the transient and steady-state frequency, even though the total control capacities in both cases are the same.

[0075] In contrast to the optimal frequency problem discussed above in SECTION 1, a similar optimization problem, the optimal load problem is discussed below in SECTION 2.

Section 2

Node Controllers for Optimal Load Control

[0076] A node controller in accordance with an embodiment of the invention is shown in FIG. **8**. In many embodiments, node controller **800** can perform calculations at a node in a power distribution network in a manner similar to the node controller described above with respect to FIG. **3**. The node controller includes at least one processor **802**, an I/O interface **804**, and memory **806**. The at least one processor **802**, when configured by software stored in memory, can perform calculations on and make changes to data passing through the I/O interface as well as to data stored in memory. In many embodiments, the memory **806** includes software including load control application **808** as well as aggregate controllable load **810**, power network dynamics parameters **812**, and dynamic load control parameters **814**. The load control application **808** will be discussed in greater detail below and can enable the node to perform calculations to solve for optimal load control subject to line flow limits. These calculations can be performed such that power network dynamics parameters **812** and dynamic load control parameters **814** (both to be discussed in detail below) can be used together to calculate the aggregate controllable load. Although a variety of node controllers are described above with reference to FIG. **8**, any of a variety of computing systems can be utilized to control a node within a power distribution system as appropriate to the requirements of specific applications in accordance with various embodiments of the invention.

Power Network Graph Representations for OLC

[0077] In many embodiments, the following graph representation is utilized to represent at least a portion of a power distribution network. While largely similar to the graph representation used above in SECTION 1, it should be noted that SECTION 2 uses different notations. $\mathbb{R}$ can be the set of real numbers and $\mathbb{N}$ can be the set of natural numbers. Given a finite set $S\subset\mathbb{N}$, $|S|$ to denotes its cardinality. For a set of scalar numbers $a_i\in\mathbb{R}$, $i\in S$, a_S can be the column vector of the a_i components, i.e. $a_S:=(a_i,\in S)\in\mathbb{R}^{|S|}$; the subscript S is typically dropped when the set is known from the context. Similarly, for two vectors $a\in\mathbb{R}^{|S|}$ and $b\in\mathbb{R}^{|S'|}$ the column vector x can be defined as $x=(a,b)\in\mathbb{R}^{|S|+|S'|}$. Given any matrix A, its transpose can be denoted as A^T and the ith row of A can be denoted as A_i. A_S can be used to denote the sub matrix of A composed only of the rows A_i with $i\in S$. The diagonal matrix of a sequence $\{a_i, i\in S\}$, is represented by $\mathrm{diag}(a_i)_{i\in S}$. Similarly, for a sequence of matrices $\{A_h, h\in S\}$, $\mathrm{blockdiag}(A_h)_{h\in S}$ can denote the block diagonal matrix. Finally, 1 (0) can be used to denote the vector/matrix of all ones (zeros), where its dimension can be understood from the context.

[0078] A power distribution network described by a directed graph $G(\mathcal{N},\epsilon)$ where $\mathcal{N}=\{1,\ldots,|\mathcal{N}|\}$ is the set of nodes (buses) and $\epsilon\subset\mathcal{N}\times\mathcal{N}$ is the set of transmission lines denoted by either e or ij such that if $ij\in\epsilon$, then $ji\notin\epsilon$.

[0079] The nodes (buses) can be partitioned $\mathcal{N}=\mathcal{G}\cup\mathcal{L}$ and $\mathcal{G}$ and $\mathcal{L}$ to indicate the set of generator and load nodes (buses) respectively. In many embodiments it can be assumed that the graph $(\mathcal{N},\epsilon)$ is connected, and additionally the following assumptions can be made which are well-justified for transmission networks: Node (bus) voltage magnitudes $|V_j|=1$ pu for $j\in\mathcal{N}$. Lines $ij\in\epsilon$ are lossless and characterized by their susceptances $B_{ij}=B_{ji}>0$. The analysis can be extended to networks with constant R/X ratio. Reactive power flows do not affect node (bus) voltage phase angles and frequencies.

[0080] In various embodiments, it can be further assumed that the node (bus) frequency ω_i and line flows P_{ij} are close to schedule values ω^0 and P_{ij}^0. In other words, $P_{ij}=P_{ij}^0+\delta P_{ij}$ and $\omega_i=\omega_0+\delta\omega_i$ with δP_{ij} and $\delta\omega_i$ small enough; without loss of generality, take $\omega_0=0$. The evolution of the transmission network is then described by

$$M_i\dot{\omega}_i = P_i^m - (d_i + \hat{d}_i) - \sum_{e\in\mathcal{E}} C_{i,e}P_e \qquad i\in\mathcal{G} \tag{17a}$$

$$0 = P_i^m - (d_i + \hat{d}_i) - \sum_{e\in\mathcal{E}} C_{i,e}P_e \qquad i\in\mathcal{L} \tag{17b}$$

$$\dot{P}_{ij} = B_{ij}(\omega_i - \omega_j) \qquad i\in\mathcal{E} \tag{17c}$$

$$\hat{d}_i = D_i\omega_i \qquad i\in\mathcal{N} \tag{17d}$$

where d_i denotes an aggregate controllable load, $\hat{d}_i=D_i\omega_i$ denotes an aggregate uncontrollable but frequency-sensitive load as well as damping loss at generator i, M_i is the generator's inertia, P_i^m is the mechanical power injected by a generator $i\in\mathcal{G}$, and $-P_i^m$ is the aggregate power consumed by constant loads for $i\in\mathcal{L}$. Finally, $C_{i,e}$ are the elements of the incidence matrix $C\in\mathbb{R}^{|\mathcal{N}|\times|\mathcal{E}|}$ of the graph $G(\mathcal{N},\epsilon)$ such that $C_{i,e}=-1$ if $e=ji\in\epsilon$, $C_{i,e}=1$ if $e=ij\in\epsilon$ and $C_{i,e}=0$ otherwise.

[0081] For notational convenience the vector for can be used whenever needed of (17), i.e.

$$M_{\mathcal{G}}\dot{\omega}_{\mathcal{G}} = P_{\mathcal{G}}^m - (d_{\mathcal{G}} + \hat{d}_{\mathcal{G}}) - C_{\mathcal{G}}P$$
$$0 = P_{\mathcal{L}}^m - (d_{\mathcal{L}} + \hat{d}_{\mathcal{L}}) - C_{\mathcal{L}}P$$

-continued

$$\dot{P} = D_B C^T \omega$$

$$\hat{d} = D\omega$$

where the matrices $C_{\mathcal{L}}$ and $C_{\mathcal{G}}$ by splitting the rows of C between generator and load nodes (buses), i.e. $C=[C_{\mathcal{G}}^T\ C_{\mathcal{L}}^T]^T$, $D=\mathrm{diag}(D_i)_{i\in\mathcal{N}}$, $D_B=\mathrm{diag}\,(B_{ij})_{ij\in\epsilon}$ and $M_{\mathcal{G}}=\mathrm{diag}(M_i)_{i\in\mathcal{G}}$.

Operational Constraints for OLC

[0082] Each control area can be indicated using k and $\mathcal{K}=\{1, \ldots, |\mathcal{K}|\}$ can indicate the set of areas. Within each area, the Automatic Generation Control (AGC) scheme seeks to restore the frequency to its nominal value as well as preserving a constant power transfer outside the area, i.e.

$$\sum_{i\in N_k}\sum_{e\in\mathcal{E}} C_{i,e}P_e = e_k^T CP = \hat{P}_k, \quad \forall\, k\in\mathcal{K}, \tag{18}$$

where $\mathcal{N}_k\subset\mathcal{N}$ is the set of nodes (buses) of area $k\in\mathcal{K}$, $e_k\in\mathbb{R}^{|\mathcal{N}|}$, $k\in\mathcal{K}$, is a vector with elements $(e_k)_i=1$ if $i\in\mathcal{N}_k$ and $(e_k)_i=0$ otherwise, $\hat{P}_k$ is the net scheduled power injection of area k.

[0083] In many embodiments, it can be shown that

$$\hat{C}:=E_{\mathcal{K}}C \tag{19}$$

with $E_{\mathcal{K}}:=[e_1 \ldots e_{|\mathcal{K}|}]^T$ and $\hat{C}\in\mathbb{R}^{|\mathcal{K}|\times|\mathcal{E}|}$, then constraint (18) can be compactly expressed using

$$\hat{C}P=\hat{P} \tag{20}$$

where $\hat{P}=(\hat{P}_k)_{k\in\mathcal{K}}\in\mathbb{R}^{|\mathcal{K}|}$. It is easy to see that $\hat{C}_{k,e}(e=ij)$ is equal to 1 if ij is an inter-area line with $i\in\mathcal{N}_k$, -1 if ij is an inter-area line with $j\in\mathcal{N}_k$, and 0 otherwise.

[0084] Finally, the thermal limit constraints are usually given by

$$\underline{P}\le P\le\overline{P} \tag{21}$$

where $\overline{P}:=(\overline{P}_e)_{e\in\epsilon}$ and $\underline{P}:=(\underline{P}_e)_{e\in\epsilon}$ represent the line flow limits, usually $\underline{P}=-\overline{P}$ so that $|P|\le\overline{P}$.

Efficient Load Control

[0085] Suppose the system (17) is in equilibrium, i.e. $\dot{\omega}_i=0$ for all i and $\dot{P}_{ij}=0$ for all ij, and at time 0, there is a disturbance, represented by a step change in the vector $P^m:=(P_i^m, i\in\mathcal{N})$, that produces a power imbalance. Then, in various embodiments, a distributed control mechanism can rebalance the system while preserving the frequency within its nominal value as well as maintaining the operational constraints described above. Furthermore, in some embodiments this mechanism can produce an efficient allocation among all the users (or loads) that are willing to adapt.

[0086] $c_i(d_i)$ and

$$\frac{\hat{d}^2}{2D_i}$$

can denote the cost or disutility of changing the load consumption by d_i and $\hat{d}_i$ respectively, which describes efficiency in terms of the loads' welfare. More precisely, a load control $(d, \hat{d})$ is efficient if it solves the following problem.

Problem 1 (WELFARE)

$$\underset{d,\hat{d}}{\text{minimize}} \quad \sum_{i\in N} c_i(d_i) + \frac{\hat{d}_i^2}{2D_i}. \tag{22}$$

subject to operational constraints.

[0087] This can balance supply and demand, i.e.

$$\sum_{i\in N}(d_i+\hat{d}_i) = \sum_{i\in N} P_i^m. \tag{23}$$

It is shown that when

$$d_i=c_i'^{-1}(\omega_i), \tag{24}$$

then (17) is a distributed primal-dual algorithm that solves (22) subject to (23).

[0088] Therefore, problem (22)-(23) can be used to forward engineering the desired node controllers, by means of primal-dual decomposition, that can rebalance supply and demand. Like primary frequency control, the system (17) and (24) suffers from the disadvantage that the optimal solution of (22)-(23) may not recover the frequency to the nominal value and satisfy the additional operational constraints described above.

[0089] A clever modification of (22)-(23) can restore the nominal frequency while maintaining the interpretation of (17) as a component of the primal-dual algorithm that solves the modified optimization problem. An additional byproduct of the formulation is that any type of linear equality and inequality constraint that the operator may require can be imposed.

Optimal Load-Side Control

[0090] The crux of a solution in various embodiments comes from including additional constraints to Problem 1 that implicitly guarantee the desired operational constraints, yet still preserves the desired structure which allows the use of (17) as part of the optimization algorithm.

[0091] Thus in several embodiments, the following modified version of Problem 1 can be used:

Problem 2 (OLC)

$$\underset{d,\hat{d},P,v}{\text{minimize}} \quad \sum_{i\in N} c_i(d_i) + \frac{\hat{d}_i^2}{2D_i}. \tag{25a}$$

subject to

$$P^m-(d+\hat{d})=CP \tag{25b}$$

$$P^m-d=L_B v \tag{25c}$$

$$\hat{C}D_B C^T v=\hat{P} \tag{25d}$$

$$\underline{P}\le D_B C^T v\le\overline{P} \tag{25e}$$

where $L_B:=CD_BC^T$ is the B_{ij}-weighted Laplacian matrix.

[0092] Although not clear at first sight, the constraint (25c) implicitly enforces that any optimal solution of OLC (d^*, $\hat{d}^*$, P^*, ν^*) will restore the frequency to its nominal value, i.e. $\hat{d}^*_i=D_i\omega^*=0$. Similarly, constraint (25d) can be used to impose (18) (or equivalently (20)) and (25e) to impose (21).

[0093] In various embodiments, the following assumptions can be utilized:

Assumption 1 (Cost function). The cost function $c_i(d_i)$ is α-strongly convex and second order continuously differentiable ($c_i \in C^2$ with $c''_i(d_i) \geq \alpha > 0$) in the interior of its domain $\mathcal{D}_i := [\underline{d}_i, \overline{d}_i] \subseteq \mathbb{R}$,

such that $c_i(d_i) \to +\infty$ whenever $d_i \to \partial\mathcal{D}$.

Assumption 2 (Slater Condition). The OLC prnblemn (25) is feasible and there is at least one feasible (d, $\hat{d}$, P, ν) such that

$d \in \mathrm{Int}\,\mathcal{D} := \Pi_{i=1}^{|\mathcal{N}|}\mathcal{D}_i$.

Properties of Optimal Solutions of OLC

[0094] The optimal solutions of OLC can have various properties. ν_i, λ_i and π_k can be used as Lagrange multipliers of constraints (25b), (25c) and (25d), and ρ_{ij}^+ and ρ_{ij}^- can be used as multipliers of the right and left constraints of (25e), respectively. In order to make the presentation more compact sometimes $x=(P, \nu) \in \mathbb{R}^{\mathcal{E}+|\mathcal{N}|}$ and $\sigma=(\nu, \lambda, \pi, \rho^+, \rho^-) \in \mathbb{R}^{2|\mathcal{N}|+|\mathcal{K}|+2|\mathcal{E}|}$, as well as $\sigma_i=(\nu_i, \lambda_i)$, $\sigma_k=(\pi_k)$ and $\sigma_{ij}=(\rho_{ij}^+, \rho_{ij}^-)$ can be used. $\rho:=(\rho^+, \rho^-)$ will also be used.

[0095] Next, the dual function $D(\sigma)$ of the OLC problem can be considered.

$$D(\sigma) = \inf_{d,\hat{d},x} L(d, \hat{d}, x, \sigma) \tag{26}$$

where

$$\begin{aligned} L(d, \hat{d}, x, \sigma) &= \sum_{i\in N}\left(c_i(d_i) + \frac{\hat{d}_i^2}{2D_i}\right) + \nu^T\left(P^m - (d+\hat{d}) - CP\right) + \\ &\quad \lambda^T(P^m - d - L_B\nu) + \pi^T\left(\hat{C}D_BC^T\nu - \hat{P}\right) + \\ &\quad \rho^{+T}(D_BC^T\nu - \overline{P}) + \rho^{-T}(\underline{P} - D_BC^T\nu) \\ &= \sum_{i\in N}\Big(c_i(d_i) - (\lambda_i + \nu_i)d_i + \frac{\hat{d}_i^2}{2D_i} - \nu_i\hat{d}_i + \\ &\quad (\nu_i + \lambda_i)P_i^m\Big) - P^TC^T\nu - \nu^T\left(L_B\lambda - CD_B\hat{C}^T\pi - \right. \\ &\quad \left. CD_B(\rho^+ - \rho^-)\right) - \pi^T\hat{P} - \rho^{+T}\overline{P} + \rho^{-T}\underline{P} \end{aligned} \tag{27}$$

[0096] Since $c_i(d_i)$ and

$$\frac{\hat{d}_i^2}{2D_i}$$

are radially unbounded, the minimization over d and $\hat{d}$ in (26) is always finite for given x and σ. However, whenever $C^T\nu \neq 0$ or $L_B\lambda - CD_B\hat{C}^T\pi - CD_B(\rho^+ - \rho^-) \neq 0$, P or ν can be modified to arbitrarily decrease (27). Thus, the infimum is attained if and only if

$$C^T\nu=0 \text{ and} \tag{28a}$$

$$L_B\lambda - CD_B\hat{C}^T\pi - CD_B(\rho^+ - \rho^-) = 0. \tag{28b}$$

[0097] Moreover, the minimum value must satisfy

$$c_i'(d_i) = \nu_i + \lambda_i \text{ and } \frac{\hat{d}_i}{D_i} = \nu_i, \quad \forall\, i \in \mathcal{N}. \tag{29}$$

[0098] Using (28) and (29) dual function can be computed

$$D(\sigma) = \begin{cases} \Phi(\sigma) & \sigma \in \tilde{N} \\ -\infty & \text{otherwise} \end{cases}, \tag{30}$$

where

$$\tilde{N} := \{\sigma \in \mathbb{R}^{2|\mathcal{N}|+|\mathcal{K}|+2|\mathcal{E}|} : (28a) \text{ and } (28b)\}$$

and the function $\Phi(\sigma)$ is decoupled in $\sigma_i=(\nu_i, \lambda_i)$, $\sigma_k=(\pi_k)$ and $\sigma_{ij}=(\rho_{ij}^+, \rho_{ij}^-)$. That is,

$$\Phi(\sigma) = \sum_{i\in N}\Phi_i(\sigma_i) + \sum_{k\in\mathcal{K}}\Phi_k(\sigma_k) + \sum_{ij\in\mathcal{E}}\Phi_{ij}(\sigma_{ij}) \tag{31}$$

where $\Phi_k(\sigma_k) = -\pi_k\hat{P}_k$, $\Phi_{ij}(\sigma_{ij}) = \rho_{ij}^-\underline{P}_{ij} - \rho_{ij}^+\overline{P}_{ij}$ and

$$\Phi_i(\sigma_i) = c_i(d_i(\sigma_i)) + (\nu_i + \lambda_i)(P_i^m - d_i(\sigma_i)) - \frac{D_i}{2}\nu_i^2, \tag{32}$$

with

$$d_i(\sigma_i) = c_i'^{-1}(\nu_i + \lambda_i). \tag{33}$$

[0099] The dual problem of the OLC (DOLC) is then given by

DOLC:

[0100]

$$\underset{\nu,\lambda,\pi,\rho}{\text{maximize}} \quad \sum_{i\in N}\Phi_i(\nu_i, \lambda_i) + \sum_{k\in\mathcal{K}}\Phi_k(\pi_k) + \sum_{ij\in\mathcal{E}}\Phi_{ij}(\rho_{ij}) \tag{34}$$

$$\text{subject to} \quad (28a) \text{ and } (28b)$$

$$\rho_{ij}^+ \geq 0, \quad \rho_{ij}^- \geq 0, \qquad ij \in \mathcal{E}$$

[0101] Clearly, DOLC is feasible (e.g. take $\sigma=0$). Then, Assumption 2 implies dual optimal is attained.

[0102] Although $D(\sigma)$ is only finite on $\tilde{N}$, $\Phi_i(\sigma_i)$, $\Phi_k(\sigma_k)$ and $\Phi_{ij}(\sigma_{ij})$ are finite everywhere. Thus sometimes the extended version of the dual function can be used (31) instead of $D(\sigma)$, knowing that $D(\sigma)=\Phi(\sigma)$ for $\sigma \in \tilde{N}$. Given any $S \subset \mathcal{N}$, $K \subset \mathcal{K}$ or $U \subset \epsilon$, define

$$\Phi_S(\sigma_S) := \sum_{i\in S}\Phi_i(\sigma_i), \quad \Phi_K(\sigma_K) := \sum_{k\in K}\Phi_k(\sigma_k)$$

$$\text{and } \Phi_U(\sigma_U) = \sum_{ij\in U}\Phi_{ij}(\sigma_{ij})$$

such that $\Phi(\sigma)=\Phi_{\mathcal{N}}(\sigma_{\mathcal{N}})+\Phi_{\mathcal{K}}(\sigma_{\mathcal{K}})+\Phi_\epsilon(\sigma_\epsilon)$.

[0103] The optimization problem has the following property: Given a connected graph $G(\mathcal{N}, \epsilon)$, then there exists a scalar ν^* such that (d^*, $\hat{d}^*$, x^*, σ^*) is a primal-dual optimal solution of OLC and DOLC if and only if $(d^*, \hat{d}^*, x^*)$ is primal feasible (satisfies (25b)-(25e)), σ^* is dual feasible (satisfies (28) and (34)),

$$\hat{d}^*_i=D_i\nu^*_i, d^*_i=c_i'^{-1}(\nu^*_i+\lambda^*_i), \nu^*_i=\nu^*,\ i\in\mathcal{N}, \tag{35}$$

and

$$\rho_{ij}^{+*}(B_{ij}(\nu_i^*-\nu_j^*)-\overline{P}_{ij})=0,\ ij\in\epsilon, \tag{36a}$$

$$\rho_{ij}^{-*}(\underline{P}_{ij}-B_{ij}(\nu^*_i-\nu^*_j))=0,\ ij\in\epsilon \tag{36b}$$

Moreover, d^*, $\hat{d}^*$, ν^* and λ^* are unique with $\nu^*=0$.

Distributed Optimal Load Control

[0104] In several embodiments, power network dynamics can be leveraged to solve the OLC problem in a distributed way. In many embodiments, the solution is based on the classical primal dual optimization algorithm that has been of great use to design congestion control mechanisms in communication networks.

[0105] Let

$$\begin{aligned} L(x,\sigma) &= \underset{d,\hat{d}}{\text{minimize}}\, L\big(d,\hat{d},x,\sigma\big) \\ &= L\big(d(\sigma),\hat{d}(\sigma),x,\sigma\big) \\ &= \Phi(\sigma) - P^TC^T\nu - \\ &\quad \nu^T\big(L_B\lambda - CD_B\hat{C}^T\pi - CD_B(\rho^+-\rho^-)\big) \end{aligned} \tag{37}$$

where $L(d, \hat{d}, x, \sigma)$ is defined as in (27), $d(\sigma):=(d_i(\sigma_i))$ and $\hat{d}(\sigma):=(\hat{d}_i(\sigma_i))$ according to (35).

[0106] The following partial primal-dual law can be proposed

$$\dot{\nu}_{\mathcal{G}} = \zeta_{\mathcal{G}}^{\nu}(P_{\mathcal{G}}^m - (d_{\mathcal{G}}(\sigma_{\mathcal{G}}) + D_{\mathcal{G}}\nu_{\mathcal{G}}) - C_{\mathcal{G}}P) \tag{38a}$$

$$0 = P_{\mathcal{L}}^m - (d_{\mathcal{L}}(\sigma_{\mathcal{L}}) + D_{\mathcal{L}}\nu_{\mathcal{L}}) - C_{\mathcal{L}}P \tag{38b}$$

$$\dot{\lambda} = \zeta^{\lambda}(P^m - d(\sigma) - L_B\nu) \tag{38c}$$

$$\dot{\pi} = \zeta^{\pi}\big(\hat{C}D_BC^T\nu - \hat{P}\big) \tag{38d}$$

$$\dot{\rho}^+ = \zeta^{\rho^+}[D_BC^T\nu - \overline{P}]^+_{\rho^+} \tag{38e}$$

$$\dot{\rho}^- = \zeta^{\rho^-}[\underline{P} - D_BC^T\nu]^+_{\rho^-} \tag{38f}$$

$$\dot{P} = \chi^P(C^T\nu) \tag{38g}$$

$$\dot{\nu} = \chi^{\nu}\big(L_B\lambda - CD_B\hat{C}^T\pi - CD_B(\rho^+-\rho^-)\big) \tag{38h}$$

where

$$\zeta_{\mathcal{G}}^{\nu} = \text{diag}(\zeta_i^{\nu})_{i\in\mathcal{G}},$$
$$\zeta^{\lambda} = \text{diag}(\zeta_i^{\lambda})_{i\in\mathcal{N}},$$
$$\zeta^{\pi} = \text{diag}(\zeta_k^{\pi})_{k\in\mathcal{K}},$$
$$\zeta^{\rho^+} = \text{diag}\big(\zeta_e^{\rho^+}\big)_{e\in\mathcal{E}},$$
$$\zeta^{\rho^-} = \text{diag}(\zeta_e^{\rho^-})_{e\in\mathcal{E}},$$

-continued

$$\chi^P = \text{diag}(\chi_e^P)_{e\in\mathcal{E}}$$

and

$$\chi^{\nu} = \text{diag}(\chi_i^{\nu})_{i\in\mathcal{N}}.$$

[0107] The operator $[\bullet]_u^+$ is an element-wise projection that maintains each element of the u(t) within the positive orthant when $\dot{u}=[\bullet]_u^+$, i.e. given any vector a with same dimension as u then $[\alpha]_u^+$ is defined element-wise by

$$[a_e]^+_{u_e} = \begin{cases} a_e & \text{if } a_e>0 \text{ or } u_e>0, \\ 0 & \text{otherwise} \end{cases}. \tag{39}$$

[0108] One property that can be used later is that given any constant vector $u^*\geq 0$, then

$$(u-u^*)^T[a]_u^+ \leq (u-u^*)^Ta \tag{40}$$

since for any pair (u_e, a_e) that makes the projection active, so $u_e=0$ and $a_e<0$ must be by definition and therefore

$$(u_e-u^*_e)a_e=-u^*_ea_e\geq 0=(u_e-u^*_e)^T[a_e]_{u_e}^+.$$

The name of the dynamic law (38) comes from the fact that

$$\frac{\partial}{\partial\nu}L(x,\sigma)^T = P^m - (d(\sigma_i)+D\nu) - CP \tag{41a}$$

$$\frac{\partial}{\partial\lambda}L(x,\sigma)^T = P^m - d(\sigma) - L_B\nu \tag{41b}$$

$$\frac{\partial}{\partial\pi}L(x,\sigma)^T = \hat{C}D_BC^T\nu - \hat{P} \tag{41c}$$

$$\frac{\partial}{\partial\rho^+}L(x,\sigma)^T = D_BC^T\nu - \overline{P} \tag{41d}$$

$$\frac{\partial}{\partial\rho^-}L(x,\sigma)^T = \underline{P} - D_BC^T\nu \tag{41e}$$

$$\frac{\partial}{\partial P}L(x,\sigma)^T = -(C^T\nu) \tag{41f}$$

$$\frac{\partial}{\partial\nu}L(x,\sigma)^T = -\big(L_B\lambda - CD_B\hat{C}^T\pi - CD_B(\rho^+-\rho^-)\big) \tag{41g}$$

[0109] Equations (38a), (38b) and (38g) show that dynamics (17) can be interpreted as a subset of the primal-dual dynamics described in (38) for the special case when $\zeta_i^{\nu}=M_i^{-1}$ and $\chi_{ij}^P=B_{ij}$. Therefore, the frequency ω_i can be interpreted as the Lagrange multiplier ν_i.

Optimal Load Control Processes

[0110] An overview of a process for calculating optimal load control is illustrated in FIG. **9**.

[0111] Process **900** includes calculating **902** power network dynamics parameters. Power network dynamics parameters will be discussed in greater detail below but can include (but are not limited to) frequency, line flows, and/or change in load consumption. Dynamic load control parameters are calculated **904**. Dynamic load control parameters are also discussed in greater detail below and can include (but are not limited to) Lagrange multipliers, and/or load consumption. It can readily be appreciated that primal network dynamics parameters and dynamic load control parameters can be a result of using a primal-dual law as described above. Aggregate controllable load can be calculated **906** using power network dynamics parameters and dynamic load control parameters. Optimal load control can be achieved **908** by adjusting the aggregate controllable load. In many embodiments, this process can occur in a distributed manner. Although a number of processes are discussed above with respect to FIG. **9**, any of a variety of different processes for controlling nodes for achieving optimal load control as appropriate to the requirements of specific applications in accordance with many embodiments of the system. Processes for adjusting aggregate controllable load in accordance with various embodiments of the invention are discussed further below.

[0112] A process for a node to adjust an aggregate controllable load is illustrated in FIG. **10**. Referring back to FIG. **8** and FIG. **9**, the process can be similar to parts of process **900** and performed by node controllers similar to node controller **800**. Process **1000** can include calculating **1002** dynamic load control parameters. Dynamic load control parameters are discussed in greater detail below and can include (but are not limited to) Lagrange multipliers, and/or load consumption. Aggregate controllable load is calculated **1004** using dynamic load control parameters and known power network dynamics parameters. In many embodiments, a shared static feedback loop can be used for parameters that must be calculated by both dynamic load control parameters and power network dynamics parameters. A shared static feedback loop is discussed further below. In many other embodiments, approximations can be made to simplify calculations of dynamic load control parameters, which may eliminate the need for a shared static feedback loop and generate a more distributed process. The aggregate controllable load is updated **1006** based on these calculations. Updating this load drives the network towards optimal load control. Although a number of processes are discussed above with respect to FIG. **10**, any of a variety of different processes for achieving distributed optimal load control as appropriate to the requirements of specific applications in accordance with various embodiments of the system.

[0113] A distributed load control scheme can be proposed that is naturally decomposed into Power Network Dynamics:

$$\dot{\omega}_{\mathcal{G}} = M_{\mathcal{G}}^{-1}\left(P_{\mathcal{G}}^{m} - \left(d_{\mathcal{G}} + \hat{d}_{\mathcal{G}}\right) - C_{\mathcal{G}}P\right) \tag{42a}$$

$$0 = P_{\mathcal{L}}^{m} - \left(d_{\mathcal{L}} + \hat{d}_{\mathcal{L}}\right) - C_{\mathcal{L}}P \tag{42b}$$

$$\dot{P} = D_B C^T \omega \tag{42c}$$

$$\hat{d} = D\omega \tag{42d}$$

and

Dynamic Load Control:

[0114]

$$\dot{\lambda}=\zeta^{\lambda}(P^{m}-d-L_{B}\nu) \tag{43a}$$

$$\dot{\pi}=\zeta^{\pi}(\hat{C}D_{B}C^{T}\nu-\hat{P}) \tag{43b}$$

$$\dot{\rho}^{+}=\zeta^{\pi^{+}}[D_{B}C^{T}\nu-\overline{P}]_{\pi^{+}}^{+} \tag{43c}$$

$$\dot{\rho}^{-}=\zeta^{\pi^{-}}[\underline{P}-D_{B}C^{T}\nu]_{\rho^{-}}^{+} \tag{43d}$$

$$\dot{\nu}=\chi^{\nu}(L_{B}\lambda-CD_{B}\hat{C}^{T}\pi-CD_{B}(\rho^{+}-\rho^{-})) \tag{43e}$$

$$d=c'^{-1}(\omega+\lambda) \tag{43f}$$

[0115] Equations (42) and (43) show how the network dynamics can be complemented with dynamic load control such that the whole system amounts to a distributed primal-dual algorithm that tries to find a saddle point on L(x, σ). It will be shown below that this system does achieve optimality as intended.

[0116] In various embodiments, the control architecture can be derived from the OLC problem. Unlike traditional observer-based controller design architecture, the dynamic load control block does not try to estimate state of the network. Instead, it drives the network towards the desired state using a shared static feedback loop, i.e. $d_i(\lambda_i+\omega_i)$.

Remark 3. One of the limitations of (43) is that in order to generate the Lagrange multipliers λ_i, $P_i^m-d_i$ must be estimated which is not easy since P_i^m cannot easily be separated from $P_i^m-D_i\omega_i$ when power injection is measured at a given node (bus) without knowing D_i. This will be addressed further in other embodiments below where a modified control scheme that can achieve the same equilibrium without needing to know D_i exactly.

Convergence Under Uncertainty

[0117] An important aspect of the implementation of the control law (43). A modified control law can be provided that solves the problem raised in Remark 3 will be described below, i.e. that does not require knowledge of D_i. It will be shown that the new control law still converges to the same equilibrium provided the estimation error of D_i is small enough.

[0118] An alternative mechanism can be proposed to compute λ_i. Instead of (43), consider the following control law:

Dynamic Load Control (2):

[0119]

$$\dot{\lambda}=\zeta^{\lambda}(M\dot{\omega}+B\omega+CP-L_{B}\nu) \tag{44a}$$

$$\dot{\pi}=\zeta^{\pi}(\hat{C}D_{B}C^{T}\nu-\hat{P}) \tag{44b}$$

$$\dot{\pi}^{+}=\zeta^{\rho^{+}}[D_{B}C^{T}{}_{\nu}-\tilde{P}]_{\rho^{+}}^{+} \tag{44c}$$

$$\dot{\rho}^{-}=\zeta^{\rho^{-}}[\underline{P}-D_{B}C^{T}\nu]_{\rho^{-}}^{+} \tag{44d}$$

$$\dot{\nu}=\chi^{\nu}(L_{B}\lambda-CD_{B}\hat{C}^{T}\pi-CD_{B}(\rho^{+}-\rho^{-})) \tag{44e}$$

$$d=c'^{-1}(\omega+\lambda) \tag{44f}$$

where M=diag $M_i)_{i\in\mathcal{N}}$ with $M_i=0$ for $i\in\mathcal{L}$, and B=diag $b_i)_{i\in\mathcal{N}}$

[0120] Notice that the only difference between (43) and (44) is that (43a) can be substituted with (44a) where now M_i only needs to be estimated for the generators, which is usually known.

[0121] The parameter b_i plays the role of D_i. In fact, whenever $b_i=D_i$ then one can use (42a) and (42b) to show that (44a) is the same as (43a). In other words, if $b_i=D_i+\delta b_i$ and $\delta B=\mathrm{diag}(\delta b_i)_{i\in\mathcal{N}}$, then using (42a) and (42b):

$$\lambda = \zeta^{\lambda}(M\dot{\omega} + B\omega + CP - L_B\nu) \tag{45}$$

-continued

$$= \zeta^{\lambda}(M\dot{\omega} + D\omega + \delta B\omega + CP - L_B v)$$

$$= \zeta^{\lambda}(P^m - d - CP + \delta B\omega + CP - L_B v)$$

$$= \zeta^{\lambda}(P^m - d + \delta B\omega - L_B v).$$

which is equal to (43a) when $\delta b_i=0$.

[0122] Using (45), the system (42) and (44) can be expressed by

$$\dot{x} = -X\frac{\partial}{\partial x}L(x, y)^T \tag{46a}$$

$$\dot{y} = Y\left[\frac{\partial}{\partial y}L(x, y)^T + g(x, y)\right]^+_{\rho} \tag{46b}$$

where

$$g(x, y) := \begin{bmatrix} 0 \\ \delta B_{\mathcal{G}} v_{\mathcal{G}} \\ \delta B_{\mathcal{L}} v^*_{\mathcal{L}}(x, y) \\ 0 \\ 0 \end{bmatrix} \begin{matrix} v_{\mathcal{G}} \\ \lambda_{\mathcal{G}} \\ \lambda_{\mathcal{L}} \\ \pi \\ \rho \end{matrix} \tag{47}$$

with matrix $\delta B_S := \mathrm{diag}(\delta b_i)_{i\in S}$.

[0123] In many embodiments, under certain conditions on b_i it can be proven that convergence to the optimal solution is preserved despite the fact that (42) with (44) is no longer a primal dual algorithm. The basic intuition behind this result is that when one uses b_i instead of D_i, the system dynamics are no longer a primal-dual law, yet provided b_i does not distant too much form D_i, the convergence properties are preserved.

Simulations of OLC

[0124] Simulations of OLC using the control scheme are illustrated. The IEEE 39 node (bus) system is illustrated in FIG. **11** to simulate the scheme. The simulation assumes that the system has two independent control areas that are connected through lines (1,2), (2,3) and (26,27). The simulated power network parameters as well as the initial stationary point (pre fault state) were obtained from the Power System Toolbox data set.

[0125] Each simulated node (bus) is assumed to have a controllable load with $\mathcal{D}_i=[-d_{max}, d_{max}]$, with $d_{max}=1$ p.u. on a 100 MVA base and disutility function

$$c_i(d_i) = \int_0^{d_i}\tan\left(\frac{\pi}{2d_{max}}s\right)ds = -\frac{2d_{max}}{\pi}\ln\left(\left|\cos\left(\frac{\pi}{2d_{max}}d_i\right)\right|\right).$$

Thus,

[0126]

$$d_i(\sigma_i) = c_i'^{-1}(\omega_i + \lambda_i) = \frac{2d_{max}}{\pi}\arctan(\omega_i + \lambda_i).$$

See FIGS. **12A-12B** for an illustration of both $c_i(d_i)$ and $d_i(\sigma_i)$.

[0127] Throughout the simulations it can be assumed that the aggregate generator damping and load frequency sensitivity parameter $D_i=0.2$ $\forall i\in\mathcal{N}$ and $\chi_i^{v}=\zeta_i^{\lambda}=\zeta_k^{\pi}=\zeta_e^{\rho^+}=\zeta_e^{\rho^-}=1$, for all $i\in\mathcal{N}$, $k\in\mathcal{K}$ and $e\in\epsilon$. These parameter values do not affect convergence, but in general they will affect the convergence rate. The values of P^m are corrected so that they initially add up to zero by evenly distributing the mismatch among the load nodes (buses). $\hat{P}$ is obtained from the starting stationary condition. $\overline{P}$ and $\underline{P}$ can initially be set so that they are not binding.

[0128] The OLC-system can be simulated as well as the swing dynamics (42) without load control ($d_i=0$), after introducing a perturbation at node (bus) 29 of $P_{29}^{m}=-2$ p.u. FIGS. **13A-13C** and FIGS. **14A-C** illustrate the evolution of the node (bus) frequencies for the uncontrolled swing dynamics (a), the OLC system without inter-area constraints (b), and the OLC with area constraints (c). FIGS. **13A-13C** illustrate frequency evolution in area 1. FIGS. **14A-14C** illustrate frequency evolution in area 2.

[0129] It can be seen that while the swing dynamics alone fail to recover the nominal frequency, the OLC controllers can jointly rebalance the power as well as recovering the nominal frequency. The convergence of OLC seems to be similar or even better than the swing dynamics, as shown in FIGS. **13A-13C** and FIGS. **14A-14C**.

[0130] Next, the action of the thermal constraints can be illustrated by adding a constraint of $\overline{P}_e=2.6$ p.u. and $\underline{P}_e=-2.6$ p.u. to the tie lines between areas. FIGS. **15A-15B** show the values of the multipliers λ_i, that correspond to the Locational Marginal Prices (LMPs), and the line flows of the tie lines for the same scenario displayed in FIGS. **13C** and **14C** i.e. without thermal limits. It can be seen that neither the initial condition, nor the new steady state can satisfy the thermal limit (shown by a dashed line). However, once thermal limits are added to the OLC scheme, FIGS. **16A-16B** show that the system converges to a new operating point that satisfies the constraints.

[0131] Finally, the conservativeness of the bound can be shown. Simulate the system (42) and (44) under the same conditions as in FIGS. **15A-15B**. B_i can be set such that the corresponding δb_is are homogeneous for every node (bus) i.

[0132] FIGS. **17A-17E** and FIGS. **18A-18E** show the evolution of the frequency ω_i and LMPs λ_i for different values of δb_i belonging to $\{-0.4, -0.21, -0.2, -0.19, 0.0\}$. Since $D_i=0.2$ at all the nodes (buses), then $\delta b_i=-0.2$ is the threshold that makes B_i go from positive to negative as δb_i decreases.

[0133] The simulations show that the system converges whenever $B_i\geq 0$ ($\delta b_i\geq -0.2$). The case when $\delta b_i=-0.2$ is of special interest. Here, the system converges, yet the nominal frequency is not restored. This is because the terms $\delta b_i\omega_i$ (45) are equal to the terms $D_i\omega_i$ in (42a)-(42b). Thus $\dot{\omega}_i$ and $\dot{\lambda}_i$ can be made simultaneously zero with nonzero w^*_i. Fortunately, this can only happen when $B_i=0$ which can be avoided since B_i is a designed parameter.

[0134] Although the present invention has been described in certain specific aspects, many additional modifications and variations would be apparent to those skilled in the art. It is therefore to be understood that the present invention can be practiced otherwise than specifically described without departing from the scope and spirit of the present invention. Thus, embodiments of the present invention should be considered in all respects as illustrative and not restrictive.

Accordingly, the scope of the invention should be determined not by the embodiments illustrated, but by the appended claims and their equivalents.

What is claimed is:

1. A node controller comprising:

a network interface;

a processor, and

a memory containing:

a frequency control application; and

a plurality of node operating parameters describing the operating parameters of a node, where the node is selected from a group consisting of at least one generator node in a power distribution network;

wherein the processor is configured by the frequency control application to:

calculate a plurality of updated node operating parameters using a distributed process to determine the updated node operating parameter using the node operating parameters, where the distributed process controls network frequency in the power distribution network; and

adjust the node operating parameters.

2. A node controller of claim **1**, wherein the node operating parameters include a node frequency.

3. A node controller of claim **1**, wherein the node operating parameters include generator node parameters.

4. A node controller of claim **1**, wherein the node operating parameters include a bounded control variable.

5. A node controller of claim **1**, wherein to calculate a plurality of updated node operating parameters using a distributed process processor using the following expression:

$$p_j^c(\omega_j) = [(c_j')^{-1}(-\omega_j)]_{\underline{p}_j}^{\overline{p}_j} \quad j \in \mathcal{G}$$

where p^c is a frequency control parameter, ω is a frequency, c is a cost or disutility function, $\underline{p}_j$ and $\overline{p}_j$ are bounds on the frequency control parameter, j is the node, and $\mathcal{G}$ is the at least one generator node.

6. A node controller comprising:

a network interface;

a processor; and

a memory containing:

a frequency control application; and

a plurality of node operating parameters describing the operating parameters of a node, where the node is selected from a group consisting of at least one load node in a power distribution network;

wherein the processor is configured by the frequency control application to:

calculate a plurality of updated node operating parameters using a distributed process to determine the updated node operating parameter using the node operating parameters, where the distributed process controls network frequency in the power distribution network; and

adjust the node operating parameters.

7. A node controller of claim **6**, wherein the node operating parameters include a node frequency.

8. A node controller of claim **6**, wherein the node operating parameters include load node parameters.

9. A node controller of claim **6**, wherein the node operating parameters include a bounded control variable.

10. A node controller of claim **6**, wherein to calculate a plurality of updated node operating parameters using a distributed process is evaluated by the processor using the following expression:

$$p_j(\omega_j) = [(c_j')^{-1}(-\omega_j)]_{\underline{p}_j}^{\overline{p}_j} \quad j \in \mathcal{L}$$

where p is a frequency control parameter, ω is a frequency, c is a cost or disutility function, $\underline{p}_j$ and $\overline{p}_j$ are bounds on the frequency control parameter, j is the node, and $\mathcal{L}$ is the at least one load node.

11. A node controller of claim **6**, wherein adjusting the node operating parameters further comprises constraining the node operating parameters within thermal limits.

12. A power distribution network, comprising:

one or more centralized computing systems;

a communications network;

a plurality of generator node controllers, where each generator node controller in the plurality of generator node controllers contains:

a generator network interface;

a generator node processor; and

a generator memory containing:

a frequency control application; and

a plurality of generator node operating parameters describing the operating parameters of a generator node in a power distribution network;

where the generator node processor is configured by the frequency control application to:

calculate a plurality of updated generator node operating parameters using a distributed process to determine the updated generator node operating parameter using the generator node operating parameters, where the distributed process controls network frequency in the power distribution network; and

adjust the generator node operating parameters; and

a plurality of load node controllers, where each load node controller in the plurality of generator node controllers contains:

a load network interface;

a load node processor; and

a load memory containing:

the frequency control application; and

a plurality of load node operating parameters describing the operating parameters of a load node in the power distribution network;

where the load node processor is configured by the frequency control application to:

calculate a plurality of updated load node operating parameters using the distributed process to determine the updated load node operating parameter using the load node operating parameters, where the distributed process controls network frequency in the power distribution network; and

adjust the load node operating parameters.

13. A power distribution network of claim **12**, wherein the generator node operating parameters include a node frequency.

14. A power distribution network of claim **12**, wherein the load node operating parameters include a node frequency.

15. A power distribution network of claim **12**, wherein the generator node operating parameters include a bounded control variable.

16. A power distribution network of claim **12**, wherein the load node operating parameters include a bounded control variable.

17. A power distribution network of claim **12**, wherein to calculate a plurality of updated generator node operating parameters using a distributed process is evaluated by the processor using the following expression:

$$p_j^c(\omega_j) = [(c_j')^{-1}(-\omega_j)]_{\underline{p}_j}^{\overline{p}_j} \quad j \in \mathcal{G}$$

where p^c is a frequency control parameter, ω is a frequency, c is a cost or disutility function, $\underline{p}_j$ and $\overline{p}_j$ are bounds on the frequency control parameter, j is the node, and $\mathcal{G}$ is the at least one generator node.

18. A power distribution network of claim **12**, wherein to calculate a plurality of updated load node operating parameters using the distributed process is evaluated by the processor using the following expression:

$$p_j(\omega_j) = [(c_j')^{-1}(-\omega_j)]_{\underline{p}_j}^{\overline{p}_j} \quad j \in \mathcal{L}$$

where p is a frequency control parameter, ω is a frequency, c is a cost or disutility function, $\underline{p}_j$ and $\overline{p}_j$ are bounds on the frequency control parameter, j is the node, and $\mathcal{L}$ is the at least one load node.

* * * * *